AEDC-TSR-78-V6
JUNE 1978

LEVEL II

2 NW

NASA/RI OA 208 AND 209 VERIFICATION STATIC-STABILITY AND CONTROL-EFFECTIVENESS TESTS OF THE SPACE SHUTTLE ORBITER VEHICLE AT MACH NUMBERS FROM 2 TO 8

J. L. Jordan
ARO, Inc., AEDC Division
A Sverdrup Corporation Company
von Kármán Gas Dynamics Facility
Arnold Air Force Station, Tennessee

Period Covered: March 21-30, 1978; March 30-April 7, 1978

APPROVED FOR PUBLIC RELEASE; DISTRIBUTION UNLIMITED.

Reviewed by:

ERVIN P. JASKOLSKI, Capt., USAF
Test Director, VKF Division
Directorate of Test Operations

Approved for Publication:
FOR THE COMMANDER:

CHAUNCEY D. SMITH, JR, Lt Colonel, USAF
Director of Test Operations
Deputy for Operations

Prepared for: National Aeronautics and Space Administration (NASA)
Johnson Space Center
Houston, Texas 77058

ARNOLD ENGINEERING DEVELOPMENT CENTER
AIR FORCE SYSTEMS COMMAND
ARNOLD AIR FORCE STATION, TENNESSEE

UNCLASSIFIED

REPORT DOCUMENTATION PAGE		READ INSTRUCTIONS BEFORE COMPLETING FORM
1. REPORT NUMBER (14) AEDC-TSR-78-V6	2. GOVT ACCESSION NO.	3. RECIPIENT'S CATALOG NUMBER
4. TITLE (and Subtitle) (4) NASA/RI 0A208 and 209 Verification Static-Stability and Control-Effectiveness Tests of the Space Shuttle Orbiter Vehicle at Mach Numbers from 2 to 8		5. TYPE OF REPORT & PERIOD COVERED Final Report - March 21 - April 7, 1978
		6. PERFORMING ORG. REPORT NUMBER
7. AUTHOR(s) (10) J. L. Jordan, ARO, Inc.		8. CONTRACT OR GRANT NUMBER(s)
9. PERFORMING ORGANIZATION NAME AND ADDRESS Arnold Engineering Development Center/DO Air Force Systems Command Arnold Air Force Station, Tennessee 37389		10. PROGRAM ELEMENT, PROJECT, TASK AREA & WORK UNIT NUMBERS Program Element 921E
11. CONTROLLING OFFICE NAME AND ADDRESS NASA-Johnson Space Center/EX33 Houston, Texas 77058		12. REPORT DATE (11) June 78
		13. NUMBER OF PAGES 45
14. MONITORING AGENCY NAME & ADDRESS (if different from Controlling Office) (12) 47 p.		15. SECURITY CLASS. (of this report) UNCLASSIFIED
		15a. DECLASSIFICATION/DOWNGRADING SCHEDULE N/A

16. DISTRIBUTION STATEMENT (of this Report)

Approved for public release; distribution unlimited.

(9) Final rept.,

17. DISTRIBUTION STATEMENT (of the abstract entered in Block 20, if different from Report)

18. SUPPLEMENTARY NOTES

Available in DDC.

19. KEY WORDS (Continue on reverse side if necessary and identify by block number)

static stability
control effectiveness
space shuttle orbiter
wind tunnel tests
supersonic flow

20. ABSTRACT (Continue on reverse side if necessary and identify by block number)

Static force tests were conducted on a 0.02-scale high-fidelity Space Shuttle Orbiter Vehicle model (SSV 102 Orbiter configuration, model 105-0) across the Mach number range from 2 to 8. Test data were obtained to verify orbiter stability and control characteristics in pitch and yaw, and to verify control effectiveness and trim limits over this Mach number range. Data were acquired from Mach 2.0 to 5.5 in increments of 0.5 at a primary free-stream unit Reynolds number of 4.5 million per ft. Data were also taken at Mach 8.0 at a

→ next page

DD FORM 1 JAN 73 1473 EDITION OF 1 NOV 65 IS OBSOLETE 042 550

UNCLASSIFIED

20. Abstract (continued)

primary free-stream unit Reynolds number of 2.3 million per ft. Data were obtained in the angle-of-attack range of -1 to 51 deg and the angle-of-sideslip range of -10 to +10 deg. Orbiter speedbrake, rudder, elevon, aileron, and body flap deflections were varied manually during the tests. Model flow-field photographs were obtained at various pitch and sideslip angles. Copies of all data with detailed test logs were transmitted to NASA and Rockwell International/Space Division under separate cover as a Final Data Package, which included a magnetic tape and a microfilm record of the data. Chrysler DATAMAN has also received magnetic tape copies of all test data. One printed copy and a microfilm record of this package were retained at AEDC.

CONTENTS

APPENDIXES

I. ILLUSTRATIONS

Figure

II. TABLES

NOMENCLATURE

A_b	Model base area, including sting cavity area, 25.9301 in.^{2}
A_c	Model base sting cavity area, 3.5467 in.^{2}
b_w	Model wing reference span, 18.734 in.
C_A	Axial-force coefficient, adjusted for sting cavity pressure, $C_{A_t} - C_{A_c}$
C_{A_b}	Base pressure axial-force coefficient, $-(p_{b_A} - p_\infty) A_b/(q_\infty \cdot S_w)$
C_{A_c}	Model balance cavity pressure axial-force coefficient, $(p_{b_A} - p_{s_c}) A_c/(q_\infty \cdot S_w)$
C_{A_f}	Forebody axial-force coefficient, $C_A - C_{A_b}$
C_{A_t}	Total axial-force coefficient, total axial force/$(q_\infty \cdot S_w)$
C_D	Drag coefficient, $C_A \cos\alpha + C_N \sin\alpha$
C_L	Lift coefficient, $C_N \cos\alpha - C_A \sin\alpha$
C_ℓ	Body axis rolling-moment coefficient, rolling moment/$(q_\infty \cdot S_w \cdot b_w)$
C_{ℓ_s}	Stability axis rolling-moment coefficient, $C_\ell \cos\alpha + C_n \sin\alpha$
C_m	Pitching-moment coefficient, pitching moment/$(q_\infty \cdot S_w \cdot C_w)$
C_N	Normal-force coefficient, normal force/$(q_\infty \cdot S_w)$
C_n	Body axis yawing-moment coefficient, yawing moment/$(q_\infty \cdot S_w \cdot b_w)$
C_{n_s}	Stability axis yawing-moment coefficient, $C_n \cos\alpha - C_\ell \sin\alpha$
C_w	Model wing reference mean aerodynamic chord, 9.496 in.
C_Y	Side-force coefficient, side force, $(q_\infty \cdot S_w)$

L/D	Lift to drag ratio ratio, C_L/C_D
M_∞	Free-stream Mach number
p_{b_A}	Average of four model base pressures, psia
p_o	Tunnel stilling chamber pressure, psia
p_{s_c}	Model balance cavity pressure, psia
p_∞	Free-stream static pressure, psia
q_∞	Free-stream dynamic pressure, psia
Re_∞, Re_∞/ft	Free-stream unit Reynolds number, 1/ft
S_w	Model wing reference area, 154.944 in.^{2}
T_o	Tunnel stilling chamber temperature, °R
X_o, Y_o, Z_o	Orbiter body coordinate stations in full-scale dimensions, in.
x, y, z	Body coordinate axes (see Fig. 6)
X_s, Y_s, Z_s	Stability coordinate axes (see Fig. 6)
α	Model angle of attack, deg
β	Model sideslip angle, deg
δ_a	Aileron deflection, $(\delta_{e_L} - \delta_{e_R})/2$, deg
δ_{bf}	Body flap deflection, positive trailing edge down, deg
δ_e	Elevon deflection, $(\delta_{e_L} - \delta_{e_R})/2$, deg
δ_{e_L}	Left elevon deflection, positive trailing edge down, deg

δ_{e_R}	Right elevon deflection, positive trailing edge down, deg
δ_r	Rudder deflection, positive trailing edge left, deg
δ_{sb}	Speedbrake deflection, angle between the inside faces of the left and right panels, always positive, deg
σ	Standard deviation, the square root of the mean-squared deviation from the mean of a variable
ϕ_i	Indicated roll angle of the model support mechanism, deg

1.0 INTRODUCTION

The work reported herein was performed at the request of the National Aeronautics and Space Administration (NASA), Johnson Space Center, Houston, Texas for the Rockwell International/Space Division, Downey, California, under Program Element 921E. The test results were obtained by ARO, Inc., AEDC Division (a Sverdrup Corporation Company), operating contractor for the AEDC, AFSC, Arnold Air Force Station, Tennessee. The test was conducted in the VKF Tunnels A and B during the periods of March 21 to 30, 1978 (Tunnel A) and March 30 to April 7, 1978 (Tunnel B) under ARO Project Number V41A/B-P5.

The tests were performed to verify the static stability and control characteristics in pitch and yaw, and the control effectiveness and trim limits of the Space Shuttle Orbiter vehicle over the Mach number range of 2 to 8. A 0.02-scale high-fidelity model of the SSV 102 Orbiter configuration (designated model 105-0) with all aerodynamically pertinent external features simulated was built for these tests. In addition to the overall test objectives, some anomolies in pitching-moment data taken in several facilities were to be studied. Secondary objectives included flow visualization shadowgraph and schlieren photographic data, which were taken at various model attitudes.

Orbiter static stability, axial-force, and base pressure data were obtained at Mach numbers from 2 to 5.5 in increments of 0.5 at a primary free-stream unit Reynolds number of 4.5 million per ft, and at Mach 8.0 at a primary free-stream unit Reynolds number of 2.3 million per ft. The total angle-of-attack range was from -1 to 51 deg with a -10 to 10 deg angle-of-sideslip range. Orbiter speedbrake, rudder, elevon, aileron, and body flap control surfaces were deflected in various combinations as primary configuration variables. Air data probes were mounted on the model nose at Mach numbers from 2.0 to 3.5 to simulate the deployment of these probes throughout this Mach range.

Copies of all data with detailed test logs were transmitted to NASA and Rockwell International under separate cover as a Final Data Package. This package included a magnetic tape and a microfilm record of the data. Chrysler DATAMAN has received magnetic tape copies of all test data. One printed copy and a microfilm record of the data package were retained at AEDC.

2.0 APPARATUS

2.1 WIND TUNNELS

The VKF Tunnels A and B (Fig. 1) are closed circuit, continuous flow, variable density wind tunnels. Each tunnel is equipped with a model injection system which allows removal of the model from the test section while the tunnel remains in operation. A description of the tunnels and air-flow calibration information may be found in Ref. 1.

Tunnel A has a 40- by 40-in. test section and an automatically driven flexible-plate-type nozzle which provides Mach numbers from 1.5 to 6.0. The tunnel operates at maximum stagnation pressures ranging from 29 psia at M_∞ = 1.5 to 200 psia at M_∞ = 6.0. Minimum operating pressures range from about one-tenth to one-twentieth of the maximum at each Mach number. The stagnation temperature can be varied from an average minimum of about 540 to a maximum of 750°R, depending upon Mach number and pressure level.

Tunnel B has axisymmetric contoured nozzles and a 50-in.-diam test section. Two interchangeable nozzles are available to provide Mach numbers of 6 and 8 and the tunnel operates over a range of stagnation pressure levels from 20 to 300 psia at M_∞ = 6, and 50 to 900 psia at M_∞ = 8. A natural-gas-fired combustion heater provides stagnation temperatures up to 1350°R. The entire tunnel (throat, nozzle, test section, and diffuser) is cooled by integral, external water jackets.

2.2 MODEL

The model (Fig. 2) is a 0.02-scale replica of the Space Shuttle Orbiter Vehicle 102 and is designated Model 105-0. It was fabricated entirely of stainless steel to the March 15, 1976 numerical control lines to tolerances of 0.25-in. full scale in linear dimensions and 0.1 deg in angular dimensions of the orbiter outer model line definition. All aerodynamically pertinent external features except the Thermal Protection System (TPS) tiles are simulated, including the Main Propulsion System (MPS) nozzles which are trimmed to clear the sting support, the Reaction Control System (RCS) thruster ports in the forward fuselage and the Orbiter Maneuvering System (OMS) pods.

All control surface deflections are set manually. Full-span elevons are mounted on the double delta planform wing trailing edge. There are four separate elevon surfaces with gaps between the inboard and outboard panels. Two sets of elevons are available to speed model changes. Each elevon panel is mounted on a deflection bracket and then attached to the wing. Upper surface flipper door panels which blend the wing to the elevon at all deflections are simulated only for negative elevon deflection angles and only at Mach 2.0 to 5.5. These panels are made from Renite filler material and are not usable in the high temperature environment of Tunnel B Mach 8.0 operation. They are also unnecessary in the high pitch range covered by the Mach 8.0 testing and are replaced there with stainless steel fairings. The available elevon deflection brackets are -35, -20, -10, -5, 0, +10, and +20 deg for the left side (inboard and outboard); and -35, -30, -20, -15, -10, 0, +10, and +20 deg for the right side (inboard and outboard). The body flap is attached to the base of the orbiter with a deflection bracket. Separate brackets are provided for deflection angles of -11.7, 0, 16.3, and 22.5 degrees. Separate model components are provided for speedbrake settings of 0, 25, 55, and 87.2 deg. Each speedbrake can be pinned at rudder deflection angles of 0, 2.5, 5, 11.28, and 22.8 deg, except for the 87.2 deg speedbrake which is limited to a maximum 11.28 deg rudder deflection. All of the quoted deflection angles are nominal; the actual deflection angles were measured before the test and appear on the data. Aerodynamic sealing of control surface hinge lines has been accomplished by close tolerance fits between parts, and by application of plaster during the test. Control surface orientation and deflection sign convention is illustrated in Fig. 3.

Air data probes are mounted to the orbiter nose to simulate their deployment at Mach numbers from 2.0 to 3.5. The model weight is about 92 pounds including the balance adapter. Sketches showing the hardware used to accomplish all four wind tunnel installations for this test program are included in Fig. 4.

2.3 INSTRUMENTATION AND MEASUREMENT ACCURACY

2.3.1 Test Conditions

Tunnel A stilling chamber pressure is measured with a 15-, 60-, 150-, or a 300-psid transducer referenced to a near vacuum. Based on periodic comparisons with secondary standards, the accuracy (a bandwidth which includes 95 percent of the residuals, i.e., 2σ deviation) of these transducers is estimated to be within ±0.2 percent of reading or ±0.015 psia, whichever is greater. Stilling chamber temperature is measured with a copper-constantan thermocouple with an accuracy of ±3°F based on repeat calibrations (2σ deviation).

Tunnel B stilling chamber pressure is measured with a 200- or 1000-psid transducer referenced to a near vacuum. Based on periodic comparisons with secondary standards, the accuracy (2σ deviation) of the transducers is estimated to be within ±0.1 percent of reading or ±0.06 psia, whichever is greater for the 200-psid range and ±0.1 percent of reading or ±0.5 psi, whichever is greater for the 1000-psid range. Stilling chamber temperature measurements are made with Chromel®-Alumel® thermocouples which have an accuracy of ±(1.5°F + 0.375 percent of reading) based on repeat calibrations (2σ deviation).

2.3.2 Test Data

Model forces and moments were measured with a six-component, moment-type, strain-gage balance (4.00-Y-36-072) supplied and calibrated by VKF. Prior to the test, static loads in each plane and combined static loads were applied to the balance to simulate the range of loads and center of pressure locations anticipated during the test. The range of check loads applied and the measurement accuracies are given in the following table. The accuracies represent the bands of 95 percent (2σ deviation) of the measured residuals, based on differences between the applied loads and the corresponding values calculated from the balance calibration equations included in the final data reduction.

Component	Balance Design Loads	Calibration Load Range	Range of Static Loads	Measurement Accuracy
Normal force, lb	±1500	±1500	±1500	±3.75
Pitching moment,* in.-lb	±7575	±7575	±6700	±18.95
Side force, lb	±1000	±1000	±300	±3.00
Yawing moment,* in.-lb	±5050	±5050	±1670	±12.65
Rolling moment, in.-lb	±800	±800	±800	±3.90
Axial force, lb	0 →300	0→300	0→300	±0.75

*About balance forward moment bridge.

The transfer distances from the balance forward moment bridge to the model moment reference location were -2.472 in. along the longitudinal axis and 0.5 in. along the vertical axis and were measured to an estimated accuracy of ±0.005 in.

The balance cavity pressure and five model base pressures were measured with 15-psid transducers referenced to a near vacuum in Tunnel A (Mach 2.0 to 5.5). Based on periodic comparisons with secondary standards, the accuracy of these transducers is estimated to be within ±0.15 percent of pressure or ±0.003 psia, whichever is greater.

In Tunnel B (Mach 8.0), these pressures were measured with 1-psid transducers referenced to a near vacuum. Based on periodic comparisons with secondary standards, the accuracy of these transducers is estimated to be within ±0.2 percent of pressure or ±0.003 psia, whichever is greater.

Model flow-field shadowgraph or color schlieren photographs were obtained on most configurations at selected model attitudes. The photographs were obtained with a double-pass optical flow-visualization system with a 35-in.-diam field of view in Tunnel A. The Tunnel B photographs were obtained using a single-pass optical flow-visualization system through the two 18-in.-diam test section windows.

3.0 PROCEDURE

3.1 TEST CONDITIONS

The test was conducted in Tunnel A at nominal Mach numbers from 2.0 to 5.5 in increments of 0.5 and a primary free-stream unit Reynolds number of 4.5 million per ft. In Tunnel B, the test was conducted at nominal Mach 8.0 at a primary free-stream unit Reynolds number of 2.3 million per ft. A summary of the test conditions at each Mach number is given below.

M_∞	P_o, psia	T_o, °R	q_∞, psia	p_∞, psia	Re_∞/ft x 10^{-6}
2.00	19.5	580	6.98	2.49	4.53
2.50	25.0	580	6.40	1.46	4.55
3.01	32.5	580	5.53	0.87	4.52
3.51	42.5	580	4.74	0.55	4.55
*4.02	55.0	580	3.99	0.35	4.52
4.01	24.0	580	1.76	0.16	1.98
4.02	70.0	580	5.08	0.45	5.75
4.52	71.0	580	3.42	0.24	4.54
*5.05	101.0	620	3.22	0.18	4.54
5.03	42.0	600	1.36	0.08	2.00
5.06	140.0	630	4.42	0.25	6.11
5.45	155.0	720	3.66	0.18	4.64
*7.98	510.0	1310	2.37	0.05	2.32
7.94	200.0	1220	0.95	0.02	1.03
8.00	820.0	1335	3.76	0.08	3.61
7.98	425.0	1285	1.97	0.04	2.00
7.90	105.0	1160	0.51	0.01	0.59

*These are the primary test conditions at these Mach numbers.

Test summaries showing all configurations tested and the variables for each are presented in Tables 1 to 4.

3.2 TEST PROCEDURE

Once the desired model configuration was built up, the model was injected into the tunnel at an attitude to minimize the balance loading and the possibility of tunnel blockage during injection. Static force data were taken in one of three modes of operation. During the portions of the test dedicated to flow diagnostics data acquisition, some data were taken by setting the model to the desired attitude using an inclinometer in the tunnel installation tank, locking the pitch mechanism, and taking data in the tunnel while the pitch mechanism remained locked, without pitching or rolling the model. During most of the test, however, data were taken in either a point-pause mode or a continuous-sweep mode. In the continuous-sweep mode, the model roll angle was set at either 0, ±90, or 180 deg, and the model was swept through the pitch or sideslip range at the rate of about 0.4 deg/sec in Tunnel A and about 1.0 deg/sec in Tunnel B. The data were then tabulated for the exact specified angle by averaging 16 data loops per 0.08 deg increment in Tunnel A, or 0.14 deg in Tunnel B and then interpolating. In the point-pause mode, 16 data loops were also averaged for each data point.

For point-pause type data, the model was positioned at the proper attitude using the VKF Model Attitude Control System (MACS). Generally, the model attitude was corrected for balance-sting deflections to within 0.1 deg of the requested attitude using MACS. Some data were taken in the point-pause mode without deflection corrections to obtain base and cavity pressure definition at a specific model roll orientation, or to force the model into a desired pair of roll quadrants to minimize flow nonuniformity effects on the force and moment data. Where a sideslip polar was specified at a fixed angle of attack corresponding to the pitch prebend angle, the polar was acquired in the continuous-sweep mode, and the resulting uncorrected pitch deflection was accepted. In addition, once at each Mach number, the same sideslip polar was obtained in the point-pause mode to achieve the specified pitch angle. The MACS was also used to initiate and terminate data acquisition for the continuous sweep data.

Base and cavity pressures were not measured during the continuous sweep mode because of the required stabilization time of the tunnel standard pressure systems. Normally, sufficient time was allowed prior to starting a sweep for the pressures to stabilize, so that they were valid on the initial data point of a continuous-sweep group. Base and cavity pressures were determined for the remainder of the continuous-pitch or continuous-sideslip group from a fifth-degree curve fit of point-pause pressure data at zero roll for sweeps at 0 and 180 roll, or at the same roll angle as the sweep data group for other roll angles. The pressure definition group was generally taken on a previous configuration with different control surface deflections. To account for a difference in pressure level caused by control deflections, the fifth-degree curve fits were shifted to agree with the initial point of the sweep group, prior to calculation of the base and cavity pressure coefficients. A speedbrake cavity pressure was measured when there was a non-zero speedbrake deflection. Model base and cavity pressure tap locations are illustrated in Fig. 5.

Static loadings were performed on the right elevons with the zero deflection brackets installed to determine elevon deflection constants. The results were 0.0052 deg/in.-lb for the inboard elevon surface and 0.0201 deg/in.-lb for the outboard elevon. These were considered satisfactory for this test series. The deflection constants at all other elevon angles on both wings may differ because of the variation in thickness of the individual elevon brackets.

3.3 DATA REDUCTION

The static force and moment data were obtained simultaneously utilizing the Tunnel A and B data acquisition systems. The force and moment measurements were reduced to coefficient form using the values calculated from the averaged data points and correcting for first and second order balance interaction effects. The coefficients were also corrected for model tare weight and balance-sting deflections. Model attitude, base pressure, and tunnel pressure and temperature were also calculated from the average values.

Orbiter force and moment coefficients are presented in both the body axis and stability axis systems. Pitching-, yawing-, and rolling-moment coefficients are referenced to a point on the model corresponding to full-scale orbiter stations of 1076.68 along the longitudinal axis and 375.00 along the vertical axis. This reference point is 16.814 in. from the model nose along the longitudinal axis and 2.507 in. below the cylindrical upper (cargo bay) surface along the vertical axis, in model scale. Since the model surface corresponds to the orbiter outer mold line, the actual model nose begins at a full-scale orbiter station of 236 along the longitudinal axis. The center-of-pressure location values are calculated relative to the model nose inner mold line which is located at a full-scale orbiter station of 238 along the longitudinal axis. Model wing reference area (154.944 $in.^2$) was used as the coefficient reference area. Model wing reference span (18.734 in.) was the reference length for the rolling- and yawing-moment coefficients while the wing reference mean aerodynamic chord (9.496 in.) was the pitching-moment coefficient reference length. The axes systems and positive coefficient directions are illustrated in Fig. 6.

The model total axial-force coefficient (C_{A_t}) was adjusted by the sting cavity axial-force coefficient (C_{A_c}) to the axial-force coefficient (C_A). Then C_A was adjusted by a base pressure axial-force coefficient (C_{A_b}), determined from an average of four base pressures, to the forebody axial-force coefficient (C_{A_f}). All stability axis data were reduced using C_A. Point-pause mode axial-force and stability axis data were reduced using base pressure measurements made at each data point. For continuous-sweep mode data, C_{A_b} and C_{A_c} values were determined from 5th degree least-squares curve fits of these values from point-pause data groups as described in Section 3.2. Tables 5 and 6 contain a correlation of sweep data groups to the point-pause mode data group from which the C_{A_b} and C_{A_c} curve fits were obtained.

The slopes of the side-force, yawing-moment, and rolling-moment coefficients versus sideslip angle for sideslip variation data groups were computed from linear least-squares curve fits of points from -2 to 2 deg sideslip. No slopes were computed for the pitch variation data groups since neither a trim nor a zero pitch condition normally occurred during these groups.

3.4 DATA UNCERTAINTY

The accuracy of the basic measurements (P_o and T_o) was discussed in Section 2.3. Based on repeat calibrations, these errors were found to be

$$\frac{\Delta P_o}{P_o} = 0.002 = 0.2\%, \quad \frac{\Delta T_o}{T_o} = 0.005 = 0.5\%$$

for Tunnel A, and

$$\frac{\Delta P_o}{P_o} = 0.001 = 0.1\%, \quad \frac{\Delta T_o}{T_o} = 0.004 = 0.4\%$$

for Tunnel B.

Uncertainties in the tunnel free-stream parameters and the model aerodynamic coefficients were estimated using the Taylor series method of error propagation, Eq. (1).

$$(\Delta F)^2 = \left(\frac{\partial F}{\partial X_1}\Delta X_1\right)^2 + \left(\frac{\partial F}{\partial X_2}\Delta X_2\right)^2 + \left(\frac{\partial F}{\partial X_3}\Delta X_3\right)^2 \ldots + \left(\frac{\partial F}{\partial X_n}\Delta X_n\right)^2 \qquad (1)$$

where ΔF is the absolute uncertainty in the dependent parameter $F = F(X_1, X_2, X_3 \ldots X_n)$ and X_n is the independent parameter (or basic measurement). ΔX_n is the uncertainty (error) in the independent measurement (or variable).

3.4.1 Test Conditions

The accuracy (based on 2σ deviation) of the basic tunnel parameters, P_o and T_o, (see Section 2.3) and the 2σ deviation in Mach number determined from test section flow calibrations were used to estimate uncertainties in the other free-stream properties using Eq. (1). The compared uncertainties in the tunnel free-stream conditions are summarized in the following table.

	Uncertainty, ± percent of actual value			
M_∞	M_∞	p_∞	q_∞	Re_∞/ft
2.00	0.8	2.5	0.9	1.0
2.50	0.5	1.9	1.0	1.0
3.01	0.6	2.6	1.4	1.2
3.51	0.4	1.7	1.1	1.0
4.02	0.5	2.4	1.5	1.2
4.01	0.5	2.4	1.5	1.2
4.52	0.5	2.7	1.8	1.3
5.05	0.5	3.0	2.0	1.4
5.03	0.5	3.0	2.0	1.4
5.06	0.5	3.0	2.0	1.4
5.45	0.3	1.9	1.3	1.1
7.98	0.3	1.6	1.1	1.0
7.94	0.4	2.4	1.7	1.2
8.00	0.3	1.6	1.1	1.0
7.90	0.4	2.4	1.7	1.2

3.4.2 Orbiter Aerodynamic Coefficients

The uncertainties of the orbiter aerodynamic coefficients are presented in the following table. These were established at the maximum aerodynamic loading condition using the Taylor series method of error propagation (Eq. 1) with the independent variables determined from the accuracy of the six component balance (listed in Section 2.3), the accuracy of the base pressure transducers (Section 2.3), and the uncertainties in the tunnel parameters (p_∞, q_∞) listed above.

		Maximum Parameter Uncertainty												
M_∞	Re_∞/ft x 10^{-6}	C_N	C_m	C_Y	C_n	C_ℓ	C_{A_t}	C_A	C_{A_f}	C_L	C_D	C_{n_S}	C_{ℓ_S}	L/D
2.00	4.53	0.0087	0.0021	0.0032	0.0007	0.0003	0.0015	0.0015	0.0029	0.0079	0.0055	0.0007	0.0003	0.0239
2.50	4.55	0.0116	0.0024	0.0034	0.0008	0.0003	0.0014	0.0015	0.0023	0.0099	0.0078	0.0007	0.0004	0.0224
3.01	4.52	0.0178	0.0035	0.0041	0.0009	0.0004	0.0021	0.0021	0.0031	0.0145	0.0114	0.0009	0.0005	0.0207
3.51	4.55	0.0083	0.0030	0.0044	0.0011	0.0004	0.0015	0.0016	0.0021	0.0075	0.0042	0.0011	0.0004	0.0217
4.02	4.52	0.0184	0.0046	0.0053	0.0013	0.0049	0.0024	0.0024	0.0034	0.0148	0.0115	0.0011	0.0006	0.0225
4.01	1.98	0.0222	0.0085	0.0112	0.0029	0.0009	0.0035	0.0035	0.0042	0.0182	0.0132	0.0024	0.0012	0.0423
4.02	5.75	0.0180	0.0040	0.0044	0.0010	0.0004	0.0023	0.0023	0.0033	0.0145	0.0115	0.0009	0.0005	0.0216
4.52	4.54	0.0117	0.0041	0.0061	0.0015	0.0005	0.0022	0.0022	0.0029	0.0106	0.0055	0.0014	0.0005	0.0252
5.05	4.54	0.0232	0.0057	0.0065	0.0016	0.0006	0.0031	0.0031	0.0042	0.0187	0.0144	0.0013	0.0040	0.0275
5.03	2.00	0.0283	0.0110	0.0145	0.0037	0.0011	0.0045	0.0045	0.0053	0.0233	0.0168	0.0031	0.0043	0.0602
5.06	6.11	0.0226	0.0048	0.0050	0.0012	0.0005	0.0029	0.0029	0.0040	0.0181	0.0142	0.0010	0.0040	0.0232
5.45	4.64	0.0089	0.0039	0.0055	0.0014	0.0004	0.0017	0.0017	0.0021	0.0082	0.0041	0.0013	0.0005	0.0267
7.98	2.32	0.0248	0.0071	0.0082	0.0021	0.0008	0.0027	0.0027	0.0033	0.0150	0.0204	0.0015	0.0013	0.0421
7.94	1.03	0.0427	0.0159	0.0204	0.0053	0.0017	0.0058	0.0058	0.0065	0.0263	0.0347	0.0036	0.0031	0.1029
8.00	3.61	0.0234	0.0054	0.0052	0.0013	0.0007	0.0022	0.0022	0.0029	0.0143	0.0195	0.0010	0.0008	0.0288
7.98	2.00	0.0257	0.0081	0.0099	0.0025	0.0009	0.0031	0.0031	0.0035	0.0157	0.0211	0.0018	0.0015	0.0500
7.90	0.59	0.0584	0.0282	0.0380	0.0098	0.0029	0.0099	0.0099	0.0103	0.0376	0.0468	0.0067	0.0057	0.1914

The basic precision of the body axis aerodynamic coefficients was also computed using only the balance and base pressure measurement accuracies listed in Section 2.3 along with the nominal test conditions, using the assumption that the free-stream flow nonuniformity is a bias type of uncertainty which is constant for all test runs. These values therefore represent the data repeatability expected and are especially useful in detailed discrimination purposes in parametric model studies. The stability axis coefficient repeatabilities are the same as the body axis repeatabilities at zero model angle of attack. The experimental repeatability observed was generally well within the expected repeatability.

		Repeatability (±) Measured Coefficient Value							
M_∞	Re/ft x 10^{-6}	C_N	C_m	C_Y	C_n	C_ℓ	C_{A_t}	C_A	C_{A_f}
2.00	4.53	0.0035	0.0020	0.0028	0.0007	0.0002	0.0007	0.0007	0.0021
2.50	4.55	0.0038	0.0022	0.0030	0.0008	0.0002	0.0008	0.0008	0.0022
3.01	4.52	0.0044	0.0025	0.0035	0.0009	0.0003	0.0009	0.0009	0.0022
3.51	4.55	0.0051	0.0030	0.0041	0.0011	0.0003	0.0010	0.0010	0.0016
4.02	4.52	0.0061	0.0035	0.0049	0.0013	0.0004	0.0012	0.0012	0.0024
4.01	1.98	0.0138	0.0080	0.0110	0.0029	0.0008	0.0028	0.0028	0.0035
4.02	5.75	0.0048	0.0028	0.0038	0.0010	0.0003	0.0010	0.0010	0.0023
4.52	4.54	0.0071	0.0041	0.0057	0.0015	0.0004	0.0014	0.0014	0.0022
5.05	4.54	0.0075	0.0044	0.0060	0.0016	0.0004	0.0015	0.0015	0.0031
5.03	2.00	0.0178	0.0104	0.0143	0.0037	0.0011	0.0036	0.0036	0.0045
5.06	6.11	0.0055	0.0032	0.0044	0.0011	0.0003	0.0011	0.0011	0.0029
5.45	4.64	0.0066	0.0038	0.0053	0.0014	0.0004	0.0013	0.0013	0.0017
7.98	2.32	0.0102	0.0059	0.0082	0.0021	0.0006	0.0020	0.0020	0.0027
7.94	1.03	0.0255	0.0148	0.0204	0.0053	0.0015	0.0051	0.0051	0.0058
8.00	3.61	0.0064	0.0037	0.0051	0.0013	0.0004	0.0013	0.0013	0.0022
7.98	2.00	0.0123	0.0071	0.0098	0.0025	0.0007	0.0025	0.0025	0.0030
7.90	0.59	0.0475	0.0276	0.0380	0.0098	0.0028	0.0095	0.0095	0.0099

3.4.3 Model Attitude

The uncertainty in model support system pitch and roll angles as determined from tunnel sector calibrations is estimated to be ±0.1 deg in pitch and ±0.2 deg in roll. These uncertainties combined with consideration of the possible errors in model deflection calculations result in an estimated accuracy of ±0.1 deg for model angle of attack (α) and sideslip angle (β).

4.0 TEST RESULTS

The purpose of this wind tunnel test program was to obtain experimental data to verify the Space Shuttle Orbiter vehicle stability and control characteristics in pitch and yaw and to verify control effectiveness and trim limits over the Mach number range from 2 to 8. These results will aid in the determination of any final orbiter design changes and for the definition of adjustments to the "Aerodynamic Design Data Book" (Ref. 2) which is a compilation of previous test data.

A complete set of test results in the form of tabulated data with detailed test logs, a microfilm copy, magnetic tape copies, and photographic data from both tunnel entries has been transmitted to NASA-JSC (Test Sponsor) and to Rockwell International/Space Division as the Final Data Package. Magnetic tapes of all test data have also been sent to Chrysler DATAMAN. The data presented in the Final Data Package has been edited and where errors were found, the data were corrected or eliminated. The significant changes made for the final data from the preliminary data reduced on-line during the test, include the following:

1. All aerodynamic coefficients were corrected for small flow nonuniformity effects.

2. The definition of C_{A_b} was changed (see Nomenclature).

3. All base and cavity pressure ratios are zeroed after the initial loop on all sweep data groups since the measurements are invalid once the sweep has begun.

4. For all data taken in Tunnel B (Groups 1001-1185) the axial-force data were reduced using an average of the initial and final instrument zeroes because of small shifts between these values resulting from balance heating effects. These shifts were normally within the quoted balance repeatability.

5. For Tunnel B sweep groups 1011, 1013 to 1028, and 1031 to 1038 no time was allowed for base pressure stabilization on the initial data point. The C_{A_b} and C_{A_c} curve fits used to reduce the axial-force data were not shifted to match the initial point. These shifts were always very small for Tunnel B data.

6. A base pressure tube contacted the model base during Tunnel B groups 1051 to 1056 affecting the axial-force data. All axial-force and stability axis coefficients have been zeroed. The data groups pertinent to the requested test matrix within these groups were rerun and appear on the detailed test logs.

7. A few other changes because of incorrect configuration codes and control surface deflection values on the tabulated data were corrected. The data and detailed test logs now agree. Additional changes made should not affect the use of the final data.

Some typical data and several comparisons with data from Ref. 2 showing overall satisfactory agreement appear in Figs. 7 to 10. Also, Figs. 11 and 12 illustrate the agreement between the data from different prebend installations during the test. A significant quantity of repeat data was taken during the test and, although not shown, the agreement was generally well within the values given in Section 3.4.2 of this report.

5.0 REFERENCES

1. Test Facilities Handbook (Tenth Edition), "von Kármán Gas Dynamics Facility, Vol. 3," Arnold Engineering Development Center, May 1974.

2. "Aerodynamic Design Data Book - Vol. 1, Orbiter Vehicle," SD72-SH-0060-1K, Rockwell/Space Division, November 1977.

APPENDIX I

ILLUSTRATIONS

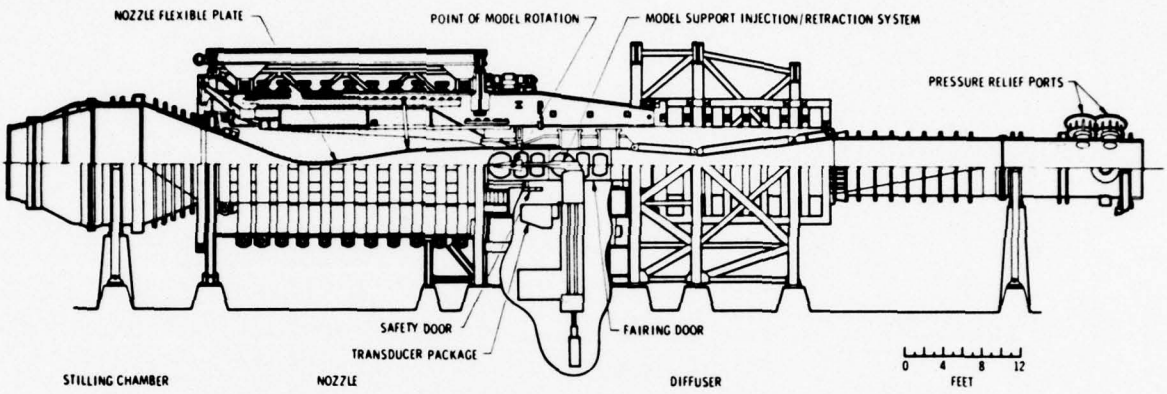

a. Tunnel A Assembly

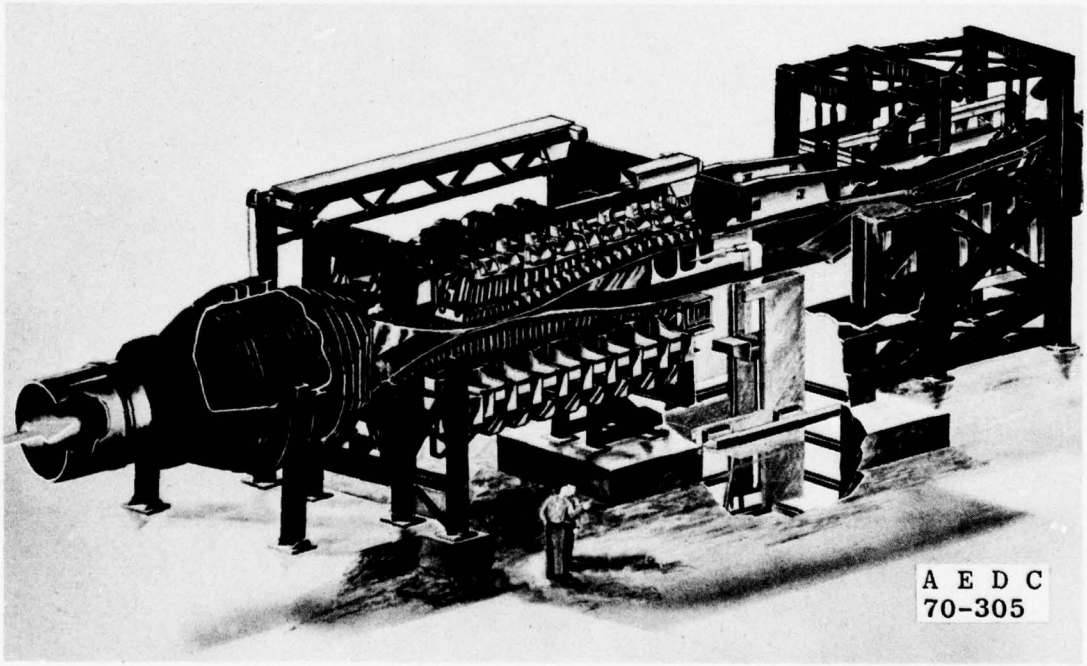

b. Tunnel A Test Section

Figure 1. VKF Wind Tunnels A and B

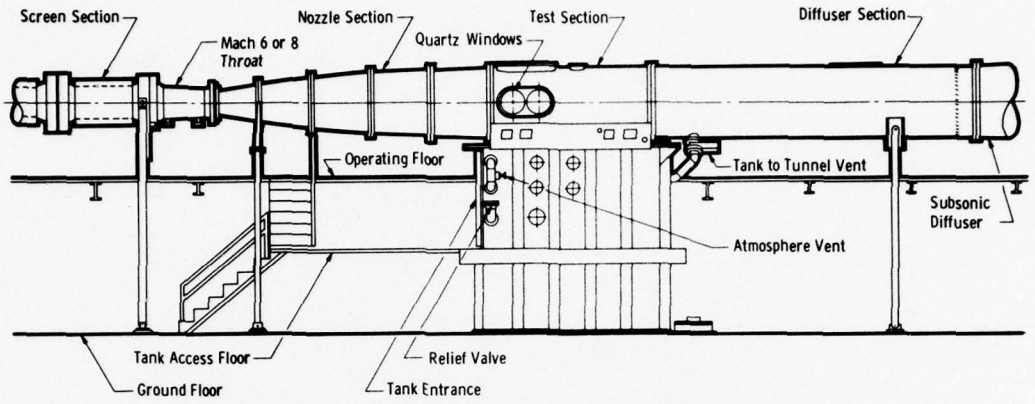

c. Tunnel B Assembly

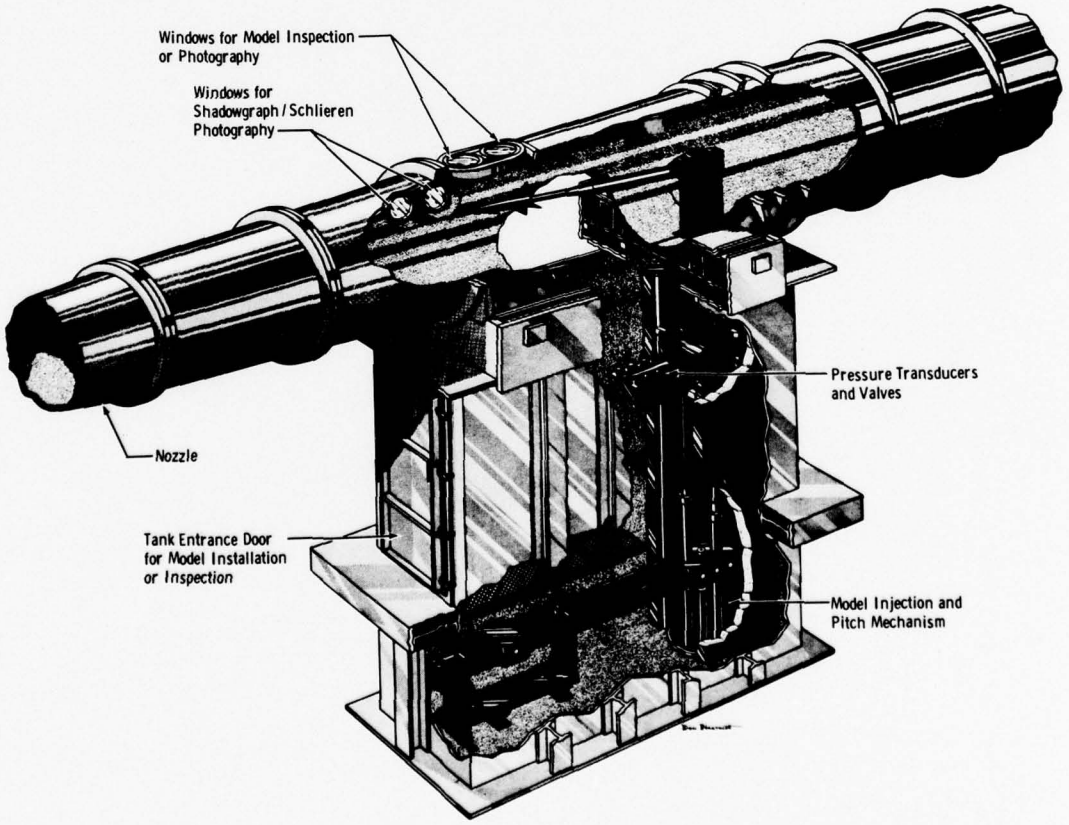

d. Tunnel B Test Section

Figure 1. Concluded

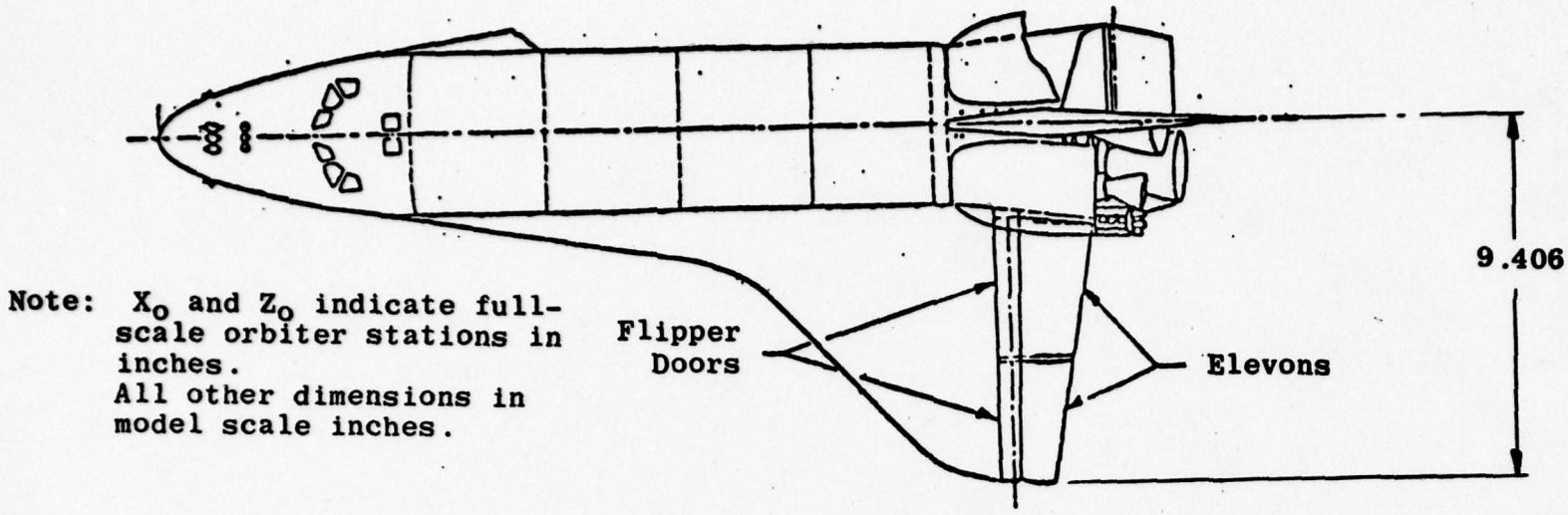

Note: X_o and Z_o indicate full-scale orbiter stations in inches.
All other dimensions in model scale inches.

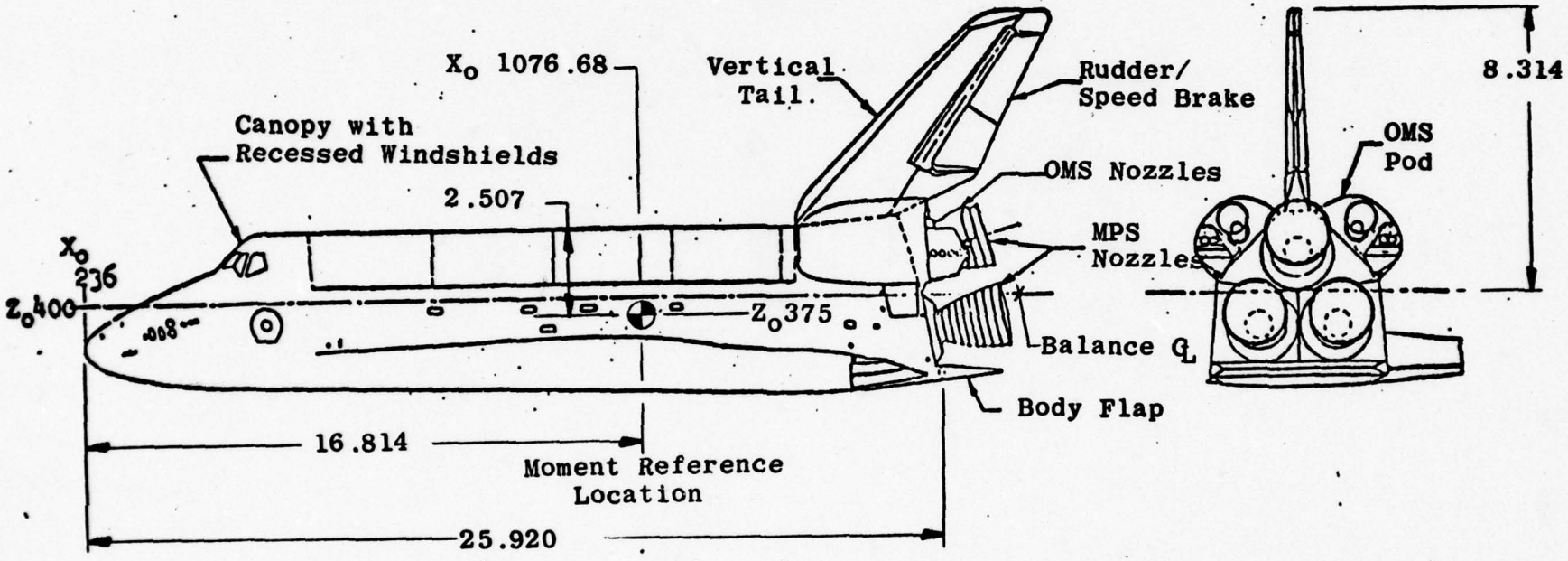

a. Overall Geometry

Figure 2. Space Shuttle Orbiter Model 105-0.

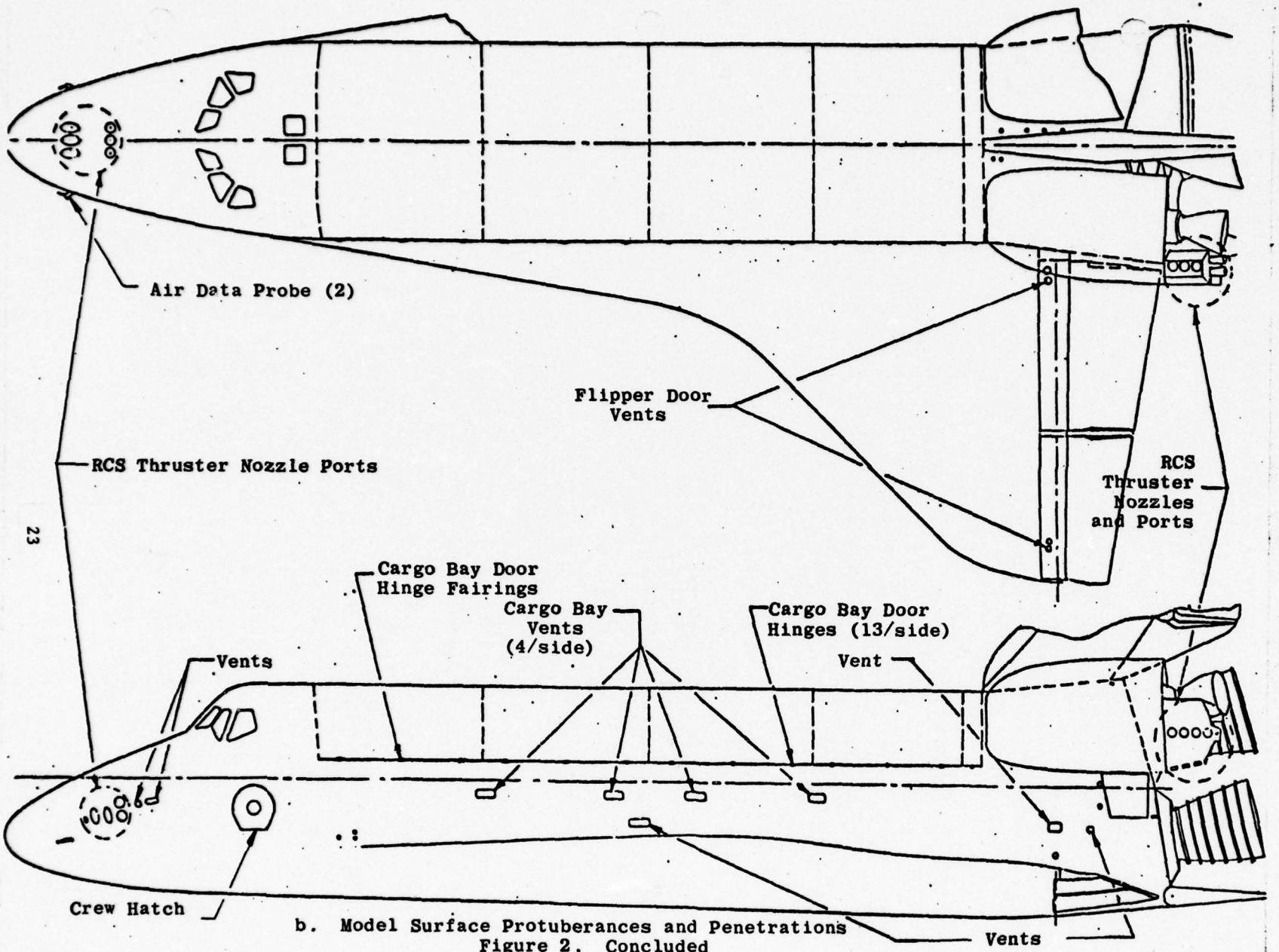

b. Model Surface Protuberances and Penetrations
Figure 2. Concluded

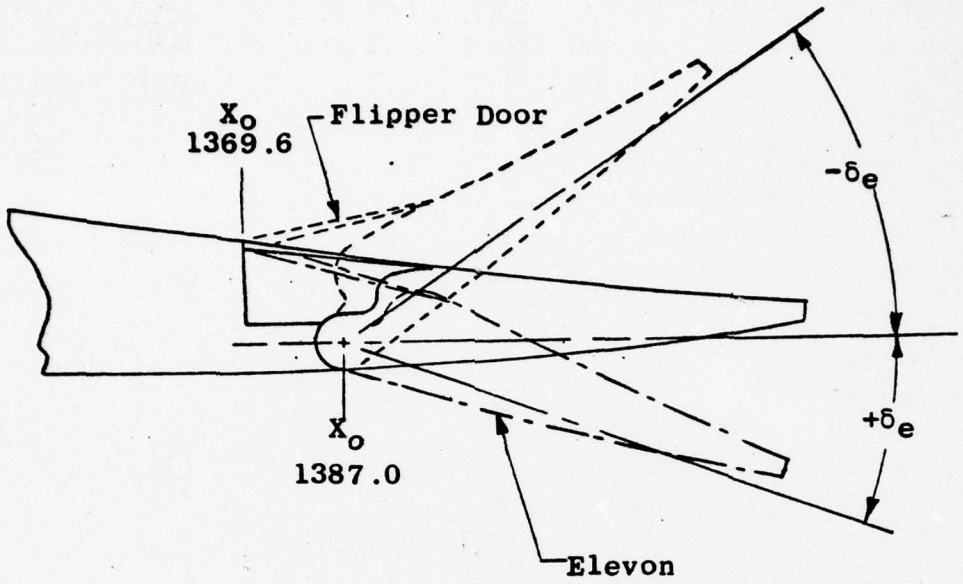

a. ELEVON DEFLECTION (δ_{eL}, δ_{eR}) SIGN CONVENTION

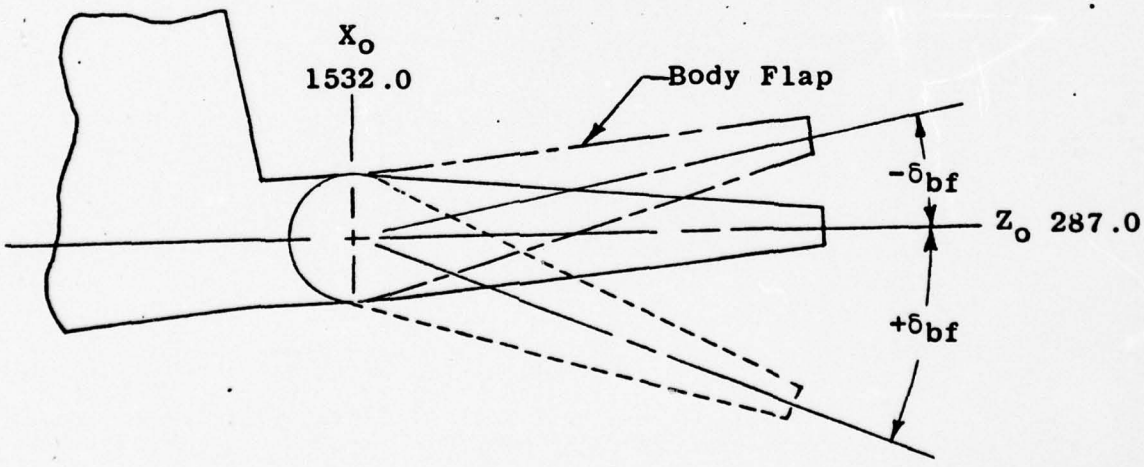

b. BODY FLAP (δ_{bf}) SIGN CONVENTION

Figure 3. Control Surface Orientation and Deflection Sign Convention

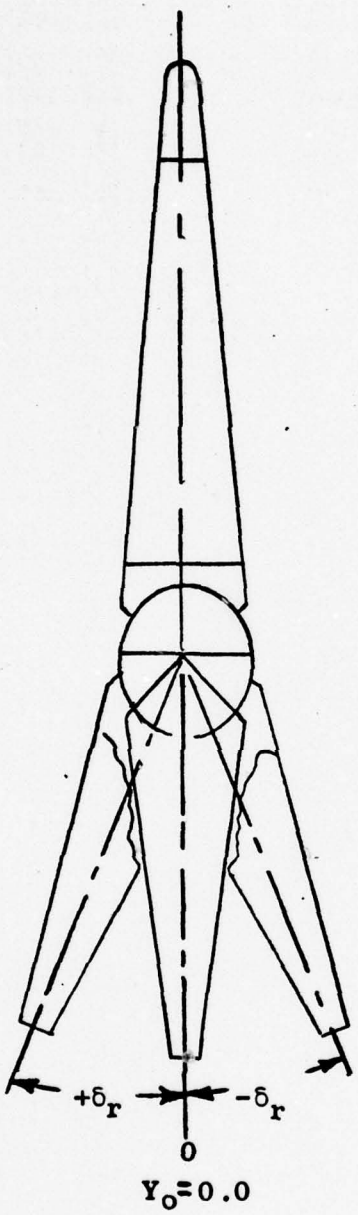

c. RUDDER DEFLECTION (δ_r) SIGN CONVENTION

Figure 3. Continued

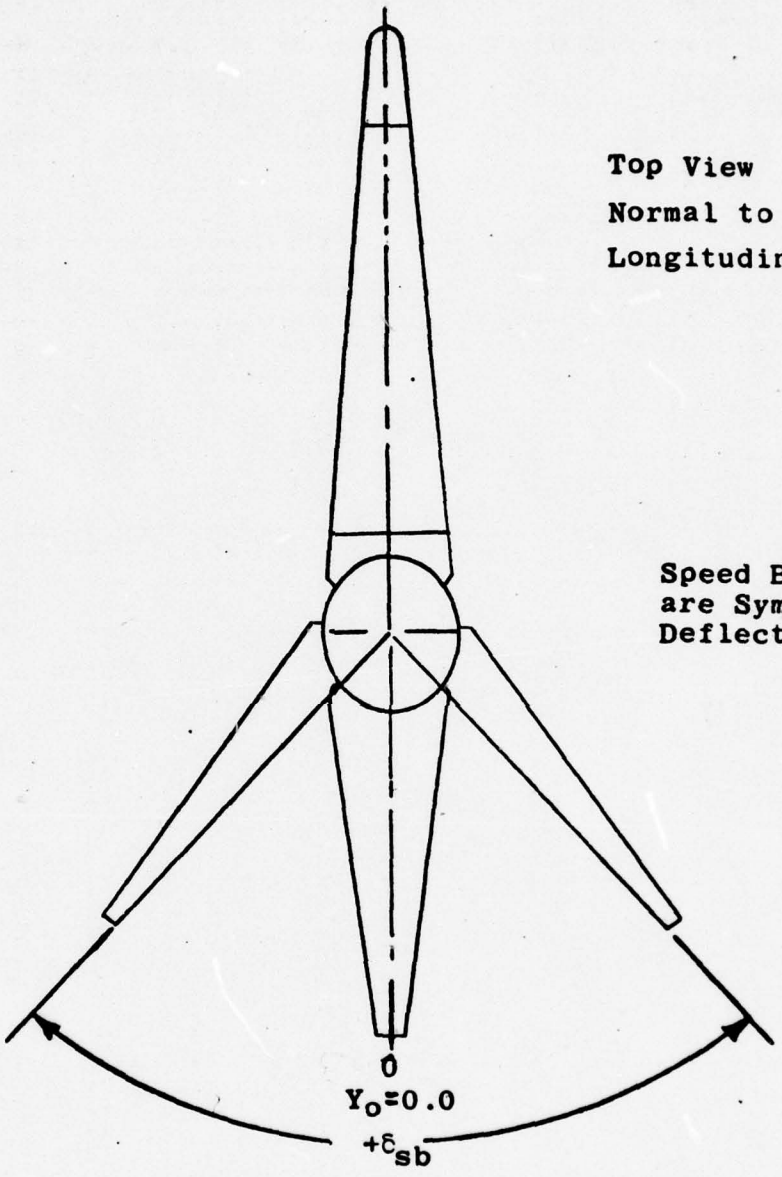

d. SPEED BRAKE DEFLECTION (δ_{sb}) SIGN CONVENTION

Figure 3. Concluded

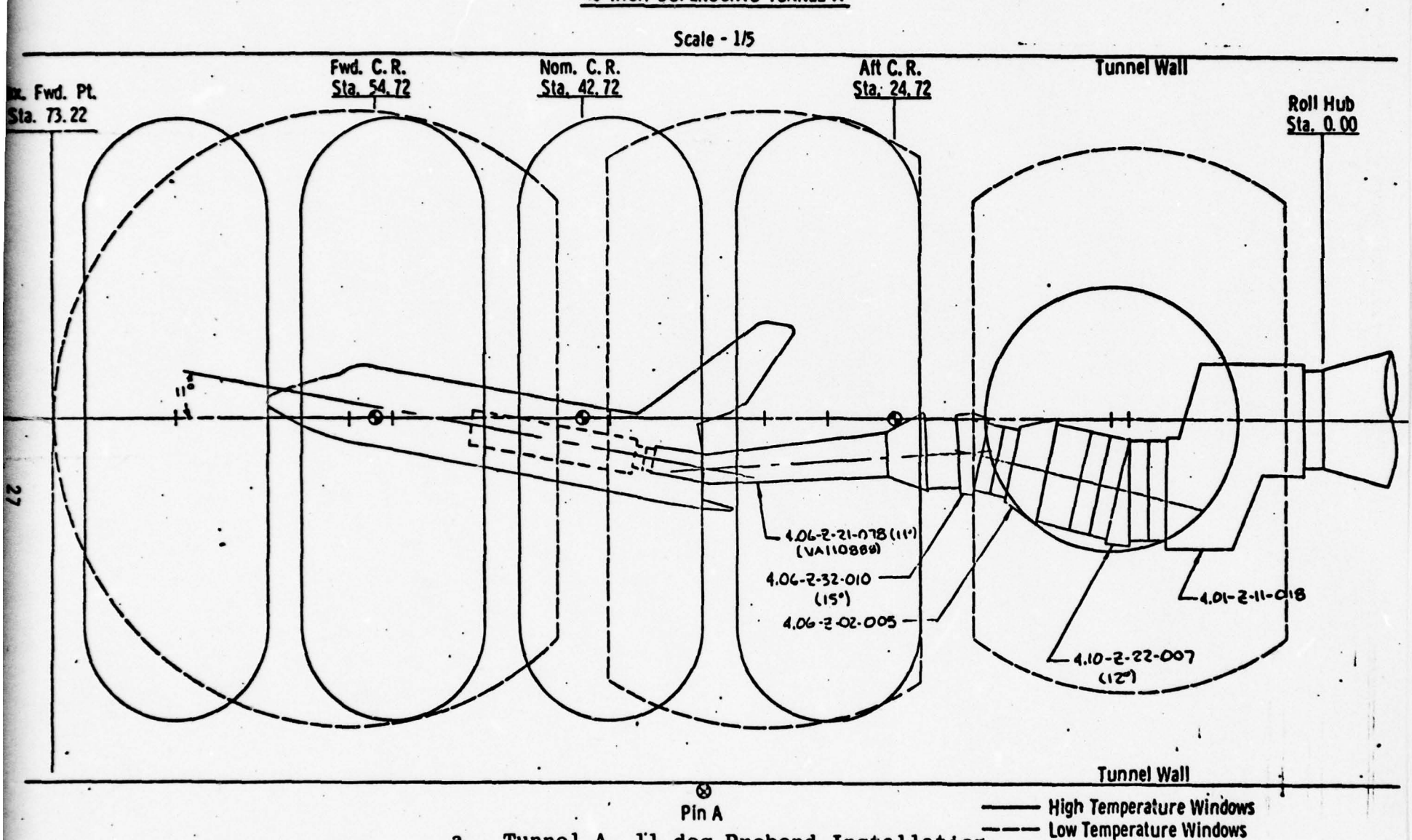

a. Tunnel A, 11 deg Prebend Installation

Figure 4. Model Installation Sketches

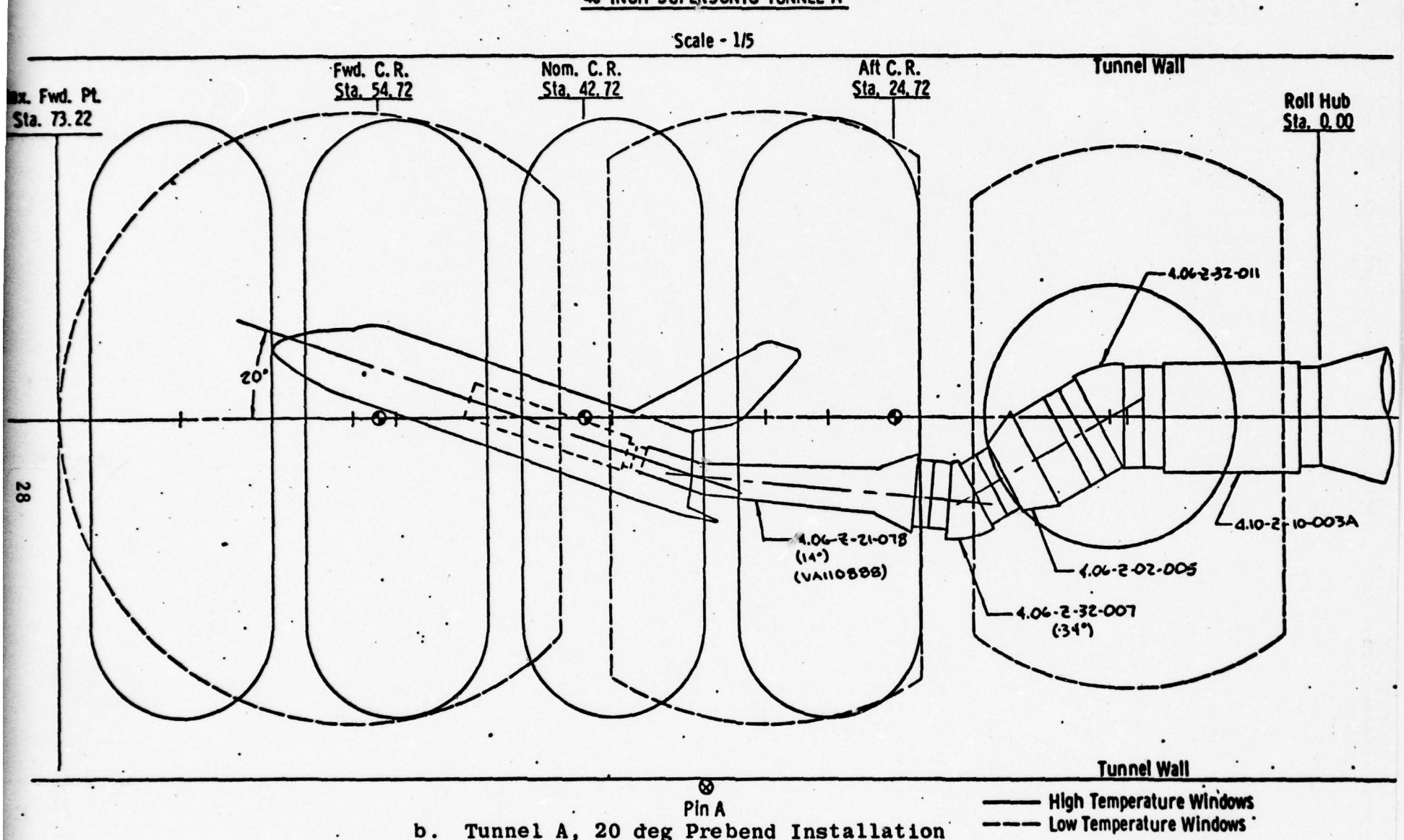

b. Tunnel A, 20 deg Prebend Installation

Figure 4. Continued

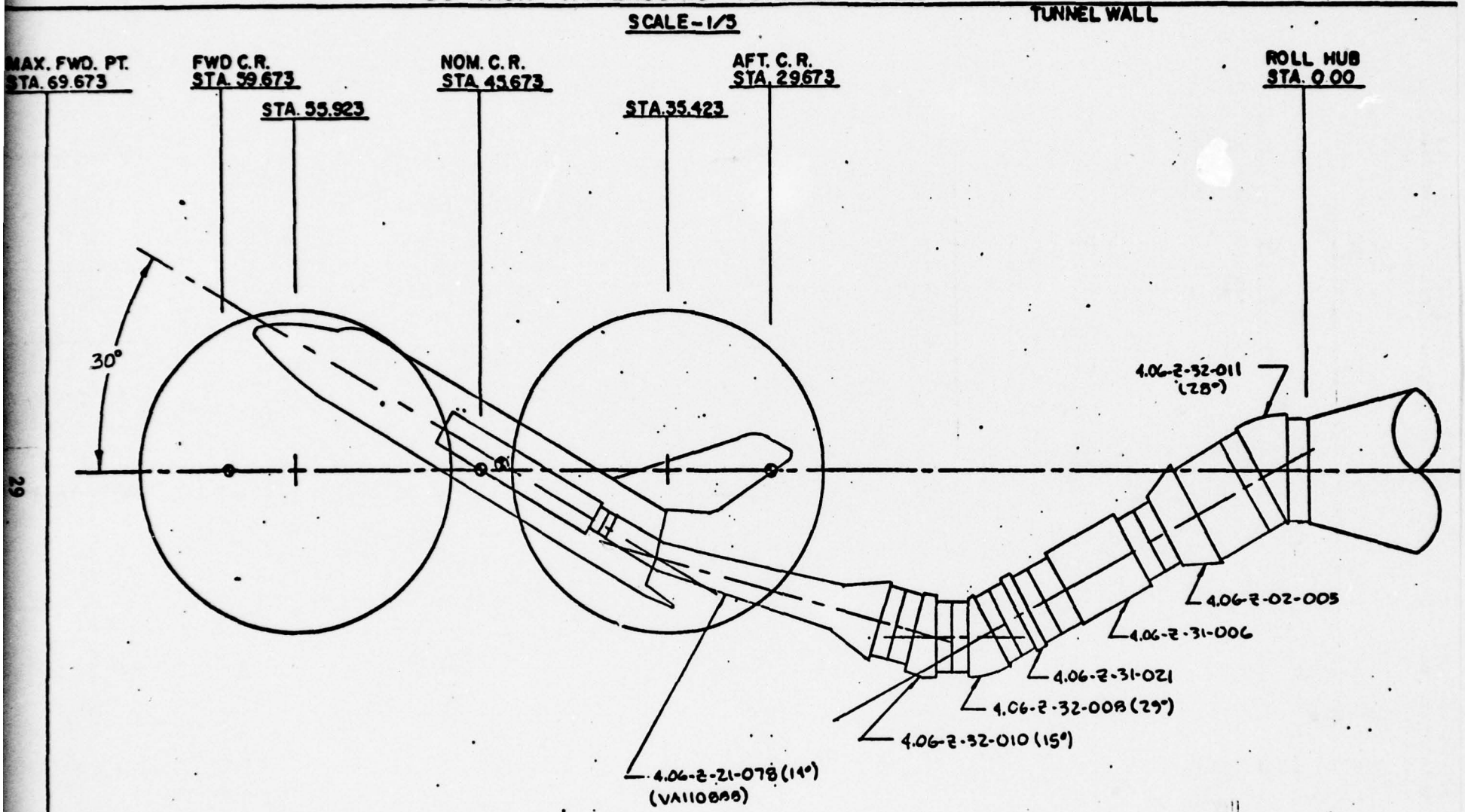

c. Tunnel B, 30 deg Prebend Installation

Figure 4. Continued

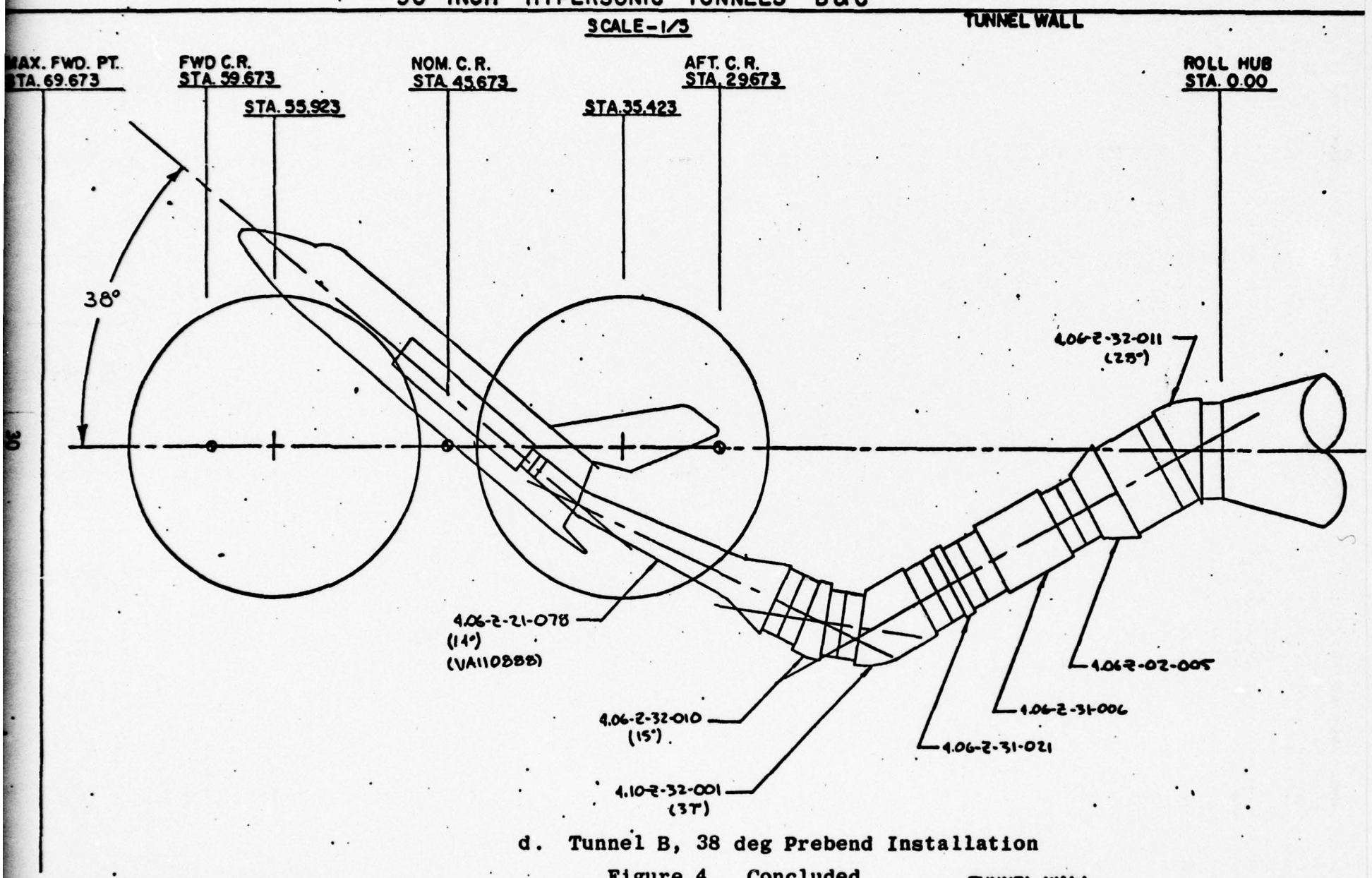

d. Tunnel B, 38 deg Prebend Installation

Figure 4. Concluded

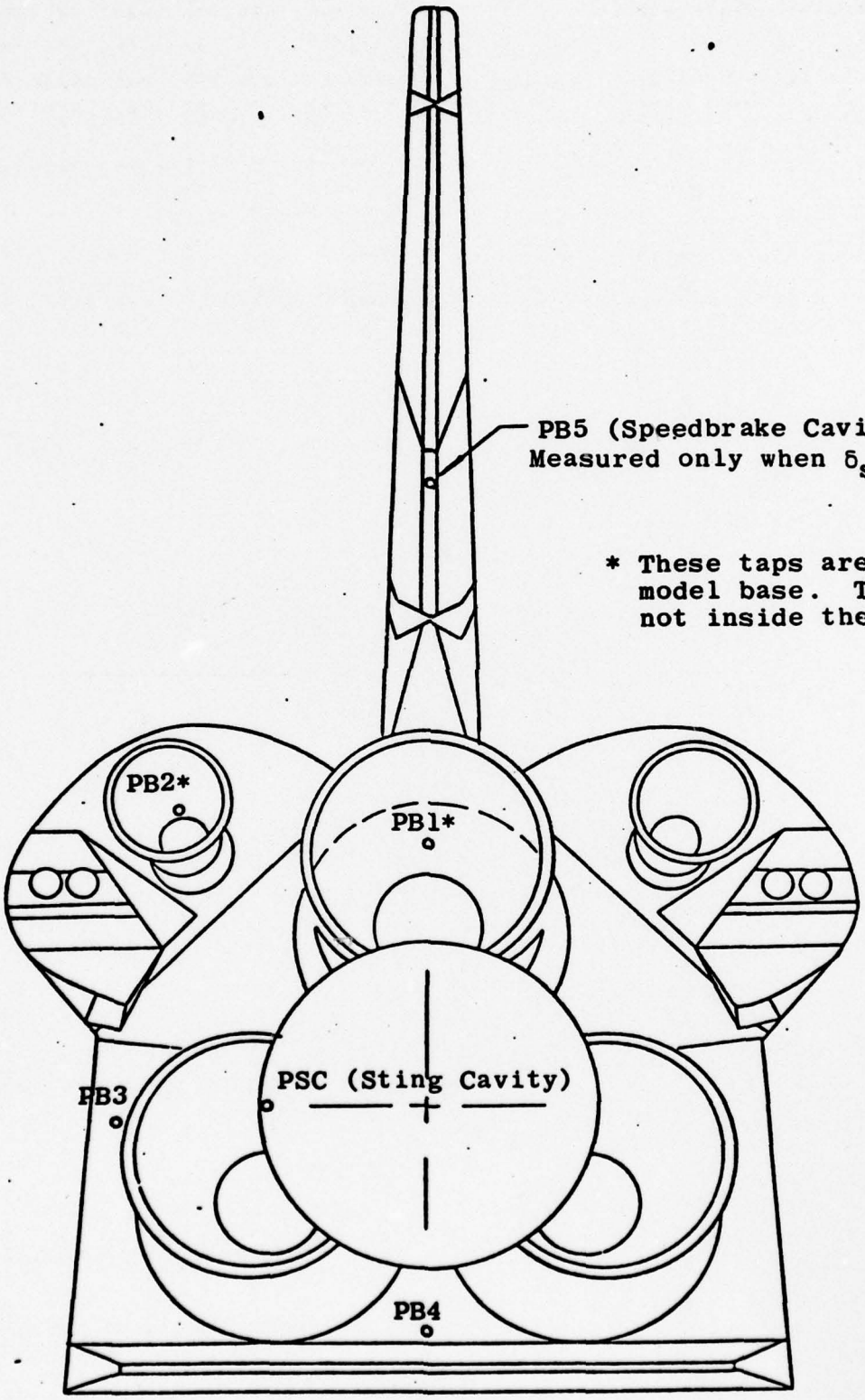

Figure 5. Base Pressure Tap Orientation

Notes:

1. Positive directions of force coefficients, moment coefficients, and angles are indicated by arrows
2. For clarity, origin of stability axes have been displaced from the center of gravity

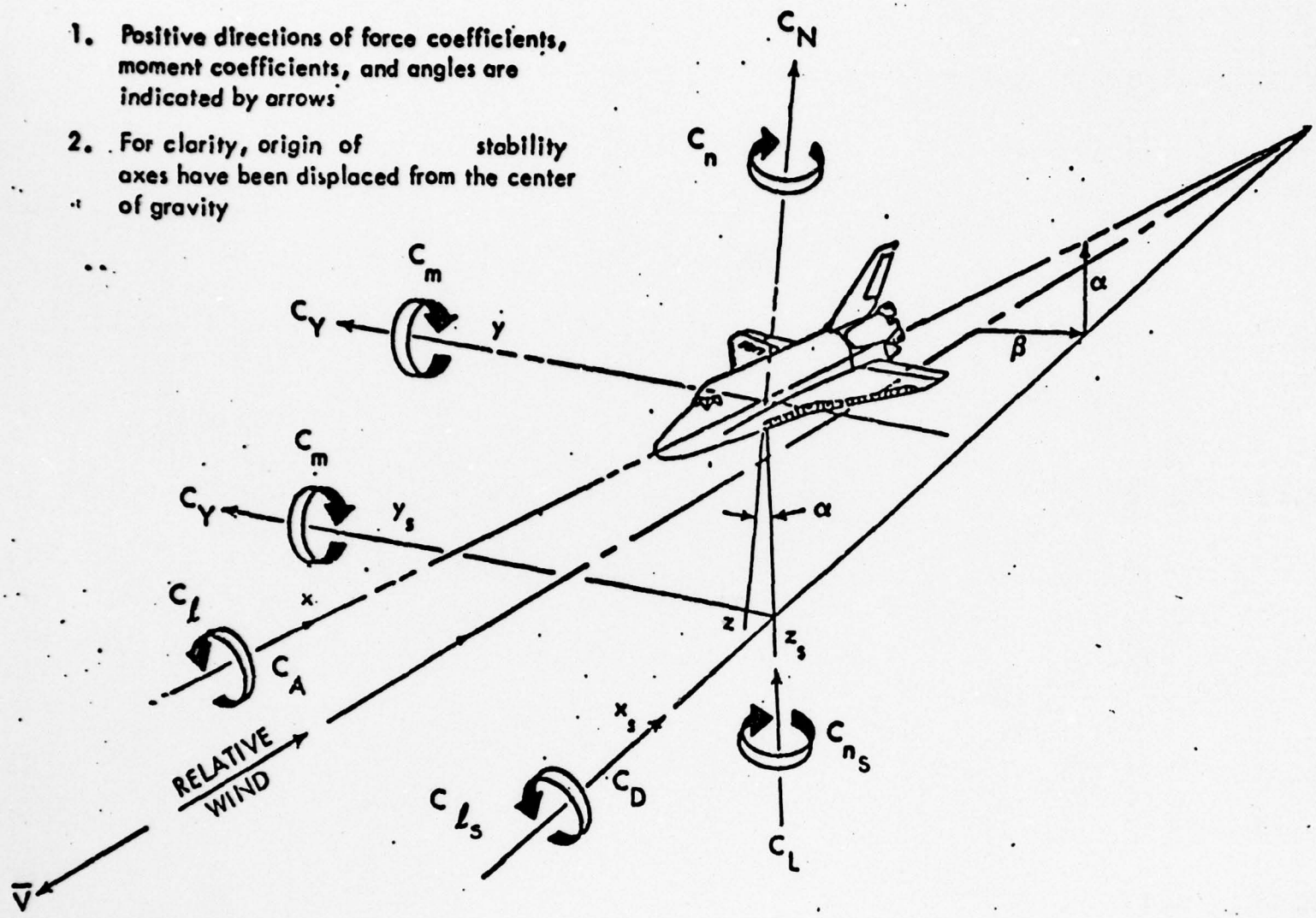

Figure 6. Axes Systems and Positive Coefficient Directions

APPENDIX II

TABLES

Table 1. OA209 (TUNNEL A) TEST SUMMARY

Re_∞/ft x 10^{-6}	Nominal Control Surface Deflections					α Range, deg	β Range, deg	Data at Nominal Mach Number							
	δ_e	δ_a	δ_{bf}	δ_{sb}	δ_r			2.0	2.5	3.0	3.5	4.0	4.5	5.0	5.5
MAX[1]	0	0	0	55	0	9 to 31	0					x		x	
2.0	↓	↓	↓	↓	↓	↓	↓					x		x	
4.5						0 to 31	-10 to + 10	x	x	x	x	x	x	x	x
↓					2.5	9 to 31						x		x	
					5					x[2]		x		x	
					11.28					x[2]		x		x	
					22.8					x[2]		x		x	
			22.5		0							x		x	
			16.3									x		x	
			-11.7							x[2]		x		x	
	20		0				0			x		x		x	
	↓		16.3				↓					x		x	
	10		0				-10 to + 10			x[2]		x		x	
	-10						↓			x[2]		x		x	
	-20						0			x		x		x	
	-35											x		x	
	↓	↓	-11.7									x		x	
	-25	5	0									x		x	
	-20	10										x		x	
	-15	5										x		x	
	-10						-10 to + 10			x[2]		x		x	
	-5						0					x		x	
	15	↓	↓	↓								x		x	
	0	0	0	↓								x		x	
	↓	↓	↓	25			-10 to + 10			x[2]		x		x	
				87.2	↓		↓					x		x	
				↓	2.5							x		x	
	0	0	0	87.2	5		-10 to + 10					x		x	
	↓	↓	↓	↓	11.28		↓					x		x	
6.0	20		16.3		0		0							x	
4.5	↓		↓		↓		↓					x		x	
↓	-35	↓	-11.7	↓	↓	↓	↓					x		x	

Note: 1. Maximum Re_∞/ft = 6.0 x 10^6 at Mach 5 and 5.75 x 10^6 at Mach 4.

2. β range was 0 at Mach 3 for these cases.

Table 2. TUNNEL A DIAGNOSTIC TEST SUMMARY

Seq NOTE	Re_∞/ft x 10^{-6}	Nominal Control Surface Deflections δ_e	δ_a	δ_{bf}	δ_{ab}	δ_r	ϕ_i Range	α Range, deg	β Range, deg	Data at Nominal Mach No. 2.0	2.5	3.0	3.5	4.0	4.5	5.0	5.5
1	4.5	0	0	0	55	0	0	0	0		x		x	x	x	x	x
1	↓	↓	↓	↓	↓	↓	180	↓	↓		x		x	x	x	x	x
							0	0 to 31		x[4]	x	x[5]	x[4]	x	x[4]	x	x[4]
							180	↓	↓	x[4]	x	x[5]	x[4]	x	x[4]	x	x[4]
							90	10.9	-10 to + 10	x	x		x	x	x	x	x
							-90	↓	↓	x	x		x	x	x	x	x
							90	20	-10 to +.10			x		x		x	
							↓	↓	↓								
							90	20.3	↓			x					
3	MAX						0	9 to 31	0					x		x	
	2.0						↓	↓	↓					x		x	
	4.5						-180 to + 180	20	↓					x		x	
	↓						-60 to 92	9 to 30	2							x	
							12 to 170	↓	↓							x	
		-10					90	20	-10 to + 10					x			
		-20		↓			0	9 to 31	0					x			
		0		16.3			90	20	-10 to + 10							x	
		↓		-11.7			↓	↓	↓							x	
		↓		↓			-90	↓	↓							x	
		10		0			90	↓	↓							x	
		0		↓	87.2		-76 to + 76	22.5	↓							x	
		↓		↓	↓		0 to -180	↓	↓							x	
	↓	20		16.3	↓	↓	0	9 to 31	0							x	
	6	↓		↓	↓	↓	↓	↓	↓							x	

Note:
1. Sector pitch mechanism remained locked during these data.
2. Air data probes were removed above Mach 3.5.
3. The maximum unit Reynolds number was 5.8 x 10^6 per foot at Mach 4.0 and 6.1 x 10^6 per foot at Mach 5.0.
4. These data covered the α range of 0 to 21 deg only.
5. These data covered the α range of 9 to 31 deg only.

Table 3

OA208 (TUNNEL B, MACH 8) TEST SUMMARY

Re_∞/ft x 10^{-6}	Nominal Control Surface Deflections					α Range, deg	β Range, deg
	δ_e	δ_a	δ_{bf}	δ_{sb}	δ_r		
3.6	0	0	0	87.2	0	17 to 43	0
1.0	↓	↓	↓	↓	↓	↓	↓
2.3	↓	↓	↓	↓	↓	17 to 51	-10 to + 10
↓	↓	↓	↓	↓	2.5	17 to 43	↓
↓	↓	↓	↓	↓	5.0	↓	↓
↓	-35	↓	↓	↓	↓	25 to 51	0
↓	0	↓	↓	↓	11.28	17 to 43	-10 to + 10
↓	-35	↓	↓	↓	↓	25 to 51	0
↓	0	↓	22.5	↓	0	17 to 51	-10 to + 10
↓	↓	↓	16.3	↓	↓	↓	↓
↓	↓	↓	-11.7	↓	↓	↓	↓
3.6	20	↓	0	↓	↓	17 to 43	0
2.3	↓	↓	↓	↓	↓	17 to 51	↓
3.6	↓	↓	16.3	↓	↓	17 to 43	↓
2.3	↓	↓	↓	↓	↓	17 to 51	↓
↓	↓	↓	-11.7	↓	↓	25 to 51	↓
↓	10	↓	0	↓	↓	17 to 51	-10 to + 10
↓	-10	↓	↓	↓	↓	↓	↓
↓	-20	↓	↓	↓	↓	17 to 43	0
↓	-35	↓	↓	↓	↓	17 to 51	↓
↓	↓	↓	-11.7	↓	↓	↓	↓
↓	-25	5	0	↓	↓	17 to 43	↓
↓	-20	10	↓	↓	↓	↓	↓
↓	-15	5	↓	↓	↓	↓	↓
↓	-10	↓	↓	↓	↓	↓	-10 to + 10
↓	↓	10	↓	↓	↓	17 to 51	0
↓	-5	5	↓	↓	↓	17 to 43	↓
↓	0	10	↓	↓	↓	17 to 51	↓
↓	5	15	↓	↓	↓	17 to 43	↓
3.6	10	10	↓	↓	↓	↓	↓
2.3	↓	↓	↓	↓	↓	17 to 51	↓
↓	15	5	↓	↓	↓	17 to 43	↓
↓	0	0	↓	55	↓	↓	-10 to + 10
3.6	20	↓	16.3	↓	↓	↓	0
2.3	-35	↓	-11.7	↓	↓	↓	↓
↓	0	↓	0	25	↓	↓	-10 to + 10
↓	↓	↓	↓	0	↓	↓	0
2.0	↓	↓	↓	↓	↓	↓	↓
0.6	↓	↓	↓	↓	↓	↓	↓
2.3	↓	↓	↓	↓	↓	↓	-10 to + 10
↓	↓	↓	↓	↓	2.5	↓	↓
↓	↓	↓	↓	↓	5.0	↓	↓
↓	↓	↓	↓	↓	11.28	↓	↓
↓	↓	↓	↓	↓	22.8	↓	↓
↓	↓	↓	22.5	↓	0	↓	↓
↓	↓	↓	16.3	↓	↓	↓	↓
↓	↓	↓	-11.7	↓	↓	↓	↓
3.6	20	↓	0	↓	↓	↓	0
↓	↓	↓	16.3	↓	↓	↓	↓
2.3	10	↓	0	↓	↓	↓	-10 to + 10
↓	-10	↓	↓	↓	↓	↓	↓
↓	-20	↓	↓	↓	↓	↓	0
↓	-35	↓	↓	↓	↓	↓	↓
↓	↓	↓	-11.7	↓	↓	↓	↓
↓	-25	5	0	↓	↓	↓	↓
↓	-20	10	↓	↓	↓	↓	↓
↓	-15	5	↓	↓	↓	↓	↓
↓	-10	↓	↓	↓	↓	↓	-10 to + 10
↓	-5	↓	↓	↓	↓	↓	0
↓	15	↓	↓	↓	↓	↓	↓

Table 4

TUNNEL B DIAGNOSTIC TEST SUMMARY (MACH 8)

Re_∞/ft x 10^{-6}	Nominal Control Surface Deflections					ϕ_i Range, deg	α Range, deg	β Range, deg
	δ_e	δ_a	δ_{bf}	δ_{sb}	δ_r			
2.3	0	0	0	0	0	0	17 to 43	0
2.0	↓	↓	↓	↓	↓	↓	↓	↓
0.6	↓	↓	↓	↓	↓	↓	↓	↓
2.3	↓	↓	↓	25	↓	↓	↓	↓
↓	↓	↓	↓	55	↓	↓	17.1[1]	↓
↓	↓	↓	↓	↓	↓	180	↓ [1]	↓
↓	↓	↓	↓	↓	↓	0	17 to 43	↓
↓	↓	↓	↓	↓	↓	180	↓	↓
↓	↓	↓	↓	↓	↓	90	30.3	-10 to + 10
↓	↓	↓	↓	↓	↓	-90	↓	↓
↓	↓	↓	↓	↓	↓	-180 to + 180	↓	0
3.6	↓	↓	↓	87.2	↓	0	17 to 43	↓
2.3	↓	↓	↓	↓	↓	↓	17 to 51	↓
↓	↓	↓	↓	↓	↓	180	25 to 51	↓
↓	↓	↓	↓	↓	↓	0	17 to 51	↓
↓	↓	↓	↓	↓	↓	-9 to -171	17 to 43	2
↓	↓	↓	↓	↓	↓	+9 to +171	↓	↓
↓	↓	↓	↓	↓	↓	-74 to -174	30	-10 to + 10
↓	↓	↓	↓	↓	↓	90	30.3	↓
↓	↓	↓	↓	↓	↓	-90	↓	↓
↓	↓	↓	↓	↓	↓	153 to -153	50.5	-6 to + 6
↓	↓	↓	↓	↓	↓	-27 to + 27	50.8	↓
1.0	↓	↓	↓	↓	↓	0	17 to 43	0
2.3	-35	↓	↓	↓	5.0	180	25 to 51	↓
3.5	20	↓	16.3	55	0	0	17 to 43	↓
↓	↓	↓	↓	87.2	↓	↓	↓	↓
↓	↓	↓	↓	↓	↓	180	↓	↓
2.3	10	↓	0	↓	↓	0	↓ [2]	↓
↓	↓	↓	↓	↓	↓	-90	30.3[2]	-10 to + 10

Note: 1. Sector pitch mechanism remained locked during these data.

2. These data were taken with both primary and alternate elevons, and with the elevon hinge lines sealed and unsealed with plaster.

Table 5

OA209 (Tunnel A) Test C_{A_b}, C_{A_c} Curve Fit

Group Correlation Summary

C_{A_b} and C_{A_c} Curve fit Group	ϕ_i of Curve fit Group	Correction Curve Applies to Groups
601	0	603,604,608,609,612,613,615,616
602	+90	605,606,610,611,617,618
621	0	622 to 625
626	+90	627 to 630
633	0	634 to 637
638	+90	639 to 642
645	0	646 to 649, 655
650	+90	651 to 654
656	0	657 to 660
663	0	664 to 667, 680 to 683, 688 to 691
668	+90	669 to 672, 684 to 687, 692 to 695
700	0	701 to 704, 709
710	0	711 to 714, 721 to 731
715	+90	716, 717
732	0	733, 734
735	0	736, 737
738	0	739 to 744
745	0	746,753,756,759,764,767,770,773,776,782,785, 788,793 to 796, 799 to 803
751	+90	755,758,762,766,769,772,775,780,784,787,791, 798,805
806	0	807,808
809	0	810,811
812	0	813 to 816, 826,829,832,837,840,843,847,853, 861,864,867,873 to 876, 879,880
823	+90	824,828,831,835,839,842,845,846,849,850,857, 863,866,870,878
883	0	884
885	0	886 to 888, 892 to 896, 899 to 901
890	+90	891,898,905
907	0	908 to 912, 916 to 918, 920,921
914	+90	915, 925

Table 6

OA208 (Tunnel B) Test C_{A_b}, C_{A_c} Curve Fit

Group Correlation Summary

C_{A_b} and C_{A_c} Curve fit Group	Φ_i of Curve Fit Group	Correction Curve Applies to Groups
1003	0	1004, 1006
1003	0	1011, 1013 to 1028 *
1046	0	1031 to 1034 *
1051	-90	1035 to 1038 *
1040	0	1041, 1042, 1130 to 1143
1043	0	1044, 1045
1046	0	1047,1048,1057,1060,1063,1066,1069,1072, 1075,1077,1079,1081,1088,1093 to 1098, 1101, 1103 to 1114,1116,1119 to 1121,1124, 1126 to 1129, 1144,1145,1147,1150,1153, 1156,1159,1160
1161	0	1162,1163
1164	0	1165,1166
1167	0	1168,1173,1180,1182,1184
1051	-90	1053,1056,1059,1062,1065,1068,1071,1074, 1076,1078,1080,1085,1091,1100,1102,1115, 1118,1123,1125,1146,1149,1152,1155,1158, 1171,1176,1181,1183,1185

*The curve fits were not shifted to match the initial data point of these continuous sweep groups because the pressures on that point were not stabilized.

APPENDIX III

SAMPLE TABULATED DATA AND NOMENCLATURE

TABULATED DATA NOMENCLATURE

AB	Model base area, including sting cavity area, 25.9301 $in.^2$
AC	Model base sting cavity area, 3.5467 $in.^2$
ALPHA	Model angle of attack, deg
ALP-I	Indicated pitch angle of the model support mechanism, deg
BETA	Model sideslip angle, deg
BW	Model wing reference span, 18.734 in.
CA	Axial-force coefficient, adjusted for sting cavity pressure, CAT - CAC
CAB	Base pressure axial-force coefficient, measured point-pause type data or calculated from a fifth-degree least-squares curve fit of point-pause data shifted to match the initial point of sweep data, $-\frac{[PBA - (P\text{-}INF)]}{Q\text{-}INF}\frac{AB}{SW}$
CAC	Model balance cavity pressure axial-force coefficient, measured during point-pause type data or calculated from a fifth-degree least-squares curve fit of point-pause data shifted to match the initial point of sweep data, $\frac{(PBA - PSC)}{Q\text{-}INF}\frac{AC}{SW}$
CAF	Forebody axial-force coefficient, CA - CAB
CAT	Total axial-force coefficient, total axial force/ Q-INF · SW
CD	Drag coefficient, CA · cos (ALPHA) + CN · sin (ALPHA)
CL	Lift coefficient, CN · cos (ALPHA) - CA · sin (ALPHA)
CLL	Body axis rolling-moment coefficient, rolling moment/ Q-INF · SW · BW
CLLS	Stability axis rolling moment coefficient, CLL · cos (ALPHA) + CLN · sin (ALPHA)
CLM	Pitching-moment coefficient, pitching moment/ Q-INF · SW · CW
CLN	Body axis yawing-moment coefficient, yawing moment/ Q-INF · SW · BW

CLNS	Stability axis yawing-moment coefficient, CLN · cos (ALPHA) - CLL sin (ALPHA)
CN	Normal-force coefficient, normal force/Q-INF · SW
CODE	Model configuration designation
CONFIG	Model configuration code, including information concerning primary/alternate elevon configurations
CW	Model wing reference mean aerodynamic chord, 9.496 in.
CY	Side-force coefficient, side force/Q-INF · SW
DCLL/DBETA	Slope of the CLL versus BETA curve at zero BETA calculated from a first degree least-squares curve fit over BETAs from -2 to 2 deg, 1/deg
DCLN/DBETA	Slope of the CLN versus BETA curve at zero BETA calculated from a first degree least-squares curve fit over BETAs from -2 to 2 deg, 1/deg
DCY/BETA	Slope of the CY versus BETA curve at zero BETA calculated from a first degree least-squares curve fit over BETAs from -2 to 2 deg, 1/deg
DEL-A	Aileron deflection, (DEL-EL - DEL-ER)/2, deg
DEL-BF	Body flap deflection, positive trailing edge down, deg
DEL-CAB	Increment applied to CAB curve fit to force agreement with the initial point of the sweep group
DEL-CAC	Increment applied to CAC curve fit to force agreement with the initial point of the sweep group
DEL-E	Elevon deflection, (DEL-EL + DEL-ER)/2, deg
DEL-EL	Left elevon deflection, positive trailing edge down, deg
DEL-ER	Right elevon deflection, positive trailing edge down, deg
DEL-R	Rudder deflection, positive trailing edge left, deg
DEL-SB	Speedbrake deflection, angle between the inside faces of the left and right panels, always positive, deg
GROUP	Data group number

LB	Orbiter body reference length, 25.806 in.
L/D	Lift to drag ratio, CL/CD
MACH	Free-stream Mach number
PBA/P-INF	Average of four base pressures normalized by P-INF, $\frac{(PB1 + PB2 + PB2 + PB4)}{4 \cdot P\text{-}INF}$
PBn/P-INF, n = 1 to 4	Base pressure 1-4 ratioed to P-INF
PB5/P-INF	Speedbrake cavity pressure ratioed to P-INF. This measurement is valid only for nonzero speedbrake deflections.
PHI-I	Indicated roll angle of the model support mechanism, deg
P-INF	Free-stream static pressure, psia
PO	Tunnel stilling chamber pressure, psia
PSC/P-INF	Model balance cavity pressure normalized by P-INF
Q-INF	Free-stream dynamic pressure, psia
RE/FT	Free-stream unit Reynolds number, 1/ft
REL	Free-stream Reynolds number based on orbiter model reference length, $\left(RE/FT\right)\left(\frac{LB}{12\ in./ft}\right)$
SW	Model wing reference area, 154.944 $in.^2$
T-INF	Free-stream static temperature, °R
TO	Tunnel stilling chamber temperature, °R
XCG	Distance from orbiter nose inner mold line to moment reference center along model X-axis, 16.774 in.
XCP/L	Model center-of-pressure location in the normal force direction relative to the model nose inner mold line, XCG/LB - (CLM · CW)/(CN · LB)

ARO, INC. - AEDC DIVISION
A SVERDRUP CORPORATION COMPANY
VON KARMAN GAS DYNAMICS FACILITY
ARNOLD AIR FORCE STATION, TENNESSEE
NASA-ROCKWELL FORCE AND MOMENT TEST OA209
0.02-SCALE OV102 MODEL 105-0
PAGE 1

DATE COMPUTED 13-APR-78
TIME COMPUTED 17:04:37
DATE RECORDED 25-MAR-78
TIME RECORDED 0:35:48
PROJECT NUMBER V41A-P5A

CONFIG	DEL-E	DEL-A	DEL-BF	DEL-SB	DEL-R	DEL-EL	DEL-ER	CODE
4126	0.00	0.00	0.00	86.81	-0.04	0.00	0.00	26

GROUP	MACH	PO	TO	Q-INF	P-INF	RE/FT	REL
780	4.02	55.0	581.7	3.990	0.353	4.497E06	9.670E06

ALP-I	PHI-I	ALPHA	BETA	PO	TO	Q-INF	P-INF	T-INF	RE/FT	REL	PSC/ P-INF	PB1/ P-INF	PB2/ P-INF	PB3/ P-INF	PB4/ P-INF	PBA/ P-INF	PB5/ P-INF
-9.93	89.90	20.12	-10.00	55.0	581.7	3.990	0.353	137.4	4.497E06	9.670E06	0.191	0.185	0.173	0.182	0.077	0.154	0.190
-8.94	89.90	20.12	-9.00	54.9	581.7	3.986	0.352	137.4	4.492E06	9.660E06	0.000	0.000	0.000	0.000	0.000	0.000	0.000
-7.95	89.90	20.12	-8.00	54.9	581.7	3.982	0.352	137.4	4.488E06	9.651E06	0.000	0.000	0.000	0.000	0.000	0.000	0.000
-6.95	89.90	20.12	-7.00	54.9	581.7	3.986	0.352	137.4	4.492E06	9.660E06	0.000	0.000	0.000	0.000	0.000	0.000	0.000
-5.96	89.90	20.12	-6.00	55.0	581.7	3.988	0.353	137.4	4.494E06	9.665E06	0.000	0.000	0.000	0.000	0.000	0.000	0.000
-4.96	89.90	20.12	-5.00	55.0	581.7	3.992	0.353	137.4	4.499E06	9.675E06	0.000	0.000	0.000	0.000	0.000	0.000	0.000
-3.97	89.90	20.12	-4.00	54.9	581.7	3.983	0.352	137.4	4.490E06	9.655E06	0.000	0.000	0.000	0.000	0.000	0.000	0.000
-2.97	89.90	20.12	-3.00	55.0	581.7	3.988	0.353	137.4	4.495E06	9.666E06	0.000	0.000	0.000	0.000	0.000	0.000	0.000
-1.97	89.90	20.12	-2.00	54.9	581.7	3.985	0.352	137.4	4.491E06	9.658E06	0.000	0.000	0.000	0.000	0.000	0.000	0.000
-0.98	89.90	20.13	-1.00	55.0	581.7	3.987	0.352	137.4	4.494E06	9.664E06	0.000	0.000	0.000	0.000	0.000	0.000	0.000
0.01	89.90	20.13	0.00	55.0	581.7	3.987	0.352	137.4	4.494E06	9.664E06	0.000	0.000	0.000	0.000	0.000	0.000	0.000
1.00	89.90	20.13	1.00	55.0	581.7	3.987	0.352	137.4	4.494E06	9.664E06	0.000	0.000	0.000	0.000	0.000	0.000	0.000
2.00	89.90	20.13	2.00	54.9	581.7	3.986	0.352	137.4	4.492E06	9.661E06	0.000	0.000	0.000	0.000	0.000	0.000	0.000
2.99	89.91	20.13	3.00	55.0	581.7	3.992	0.353	137.4	4.500E06	9.676E06	0.000	0.000	0.000	0.000	0.000	0.000	0.000
3.99	89.90	20.14	4.00	55.0	581.7	3.987	0.352	137.4	4.494E06	9.664E06	0.000	0.000	0.000	0.000	0.000	0.000	0.000
4.98	89.90	20.14	5.00	54.8	581.7	3.977	0.352	137.4	4.483E06	9.641E06	0.000	0.000	0.000	0.000	0.000	0.000	0.000
5.98	89.92	20.14	6.00	55.0	581.7	3.994	0.353	137.4	4.501E06	9.680E06	0.000	0.000	0.000	0.000	0.000	0.000	0.000
6.97	89.92	20.14	7.00	55.0	581.7	3.989	0.353	137.4	4.496E06	9.668E06	0.000	0.000	0.000	0.000	0.000	0.000	0.000
7.97	89.92	20.15	8.00	55.0	581.7	3.992	0.353	137.4	4.500E06	9.677E06	0.000	0.000	0.000	0.000	0.000	0.000	0.000
8.96	89.92	20.15	9.00	54.9	581.7	3.985	0.352	137.4	4.492E06	9.660E06	0.000	0.000	0.000	0.000	0.000	0.000	0.000
9.95	89.93	20.16	10.00	55.0	581.7	3.993	0.353	137.4	4.500E06	9.677E06	0.000	0.000	0.000	0.000	0.000	0.000	0.000

-9.93 89.90 DEL-CAB=-0.0001 DEL-CAC=-0.0000

44

Sample Tabulated Tunnel Conditions and Base Pressures

ARO, INC. - AEDC DIVISION
A SVERDRUP CORPORATION COMPANY
VON KARMAN GAS DYNAMICS FACILITY
ARNOLD AIR FORCE STATION, TENNESSEE
NASA-ROCKWELL FORCE AND MOMENT TEST OA209
0.02-SCALE OV102 MODEL 105-0
PAGE 3 DATA ADJUSTED FOR TUNNEL EFFECT

DATE COMPUTED 1-MAY-78
TIME COMPUTED 16:08:50
DATE RECORDED 25-MAR-78
TIME RECORDED 0:35:48
PROJECT NUMBER V41A-P5A

CONFIG	DEL-E	DEL-A	DEL-BF	DEL-SB	DEL-R	DEL-EL	DEL-ER	CODE
4126	0.00	0.00	0.00	86.81	-0.04	0.00	0.00	26

GROUP	MACH	PO	TO	Q-INF	P-INF	RE/FT	REL
780	4.02	55.0	581.7	3.990	0.353	4.497E06	9.670E06

ALPHA	BETA	CN	CLM	CY	CLN	CLL	CAT	CA	CAF	CAB	CAC	XCP/L	CLNS	CLLS	CL	CD	L/D
20.12	-10.00	0.5224	-0.0141	0.1193	0.0069	0.0181	0.0788	0.0789	0.0663	0.0125	-0.0001	0.660	0.0002	0.0194	0.4634	0.2537	1.826
20.12	-9.00	0.5243	-0.0149	0.1064	0.0061	0.0163	0.0781	0.0782	0.0657	0.0125	-0.0001	0.660	0.0001	0.0174	0.4654	0.2538	1.834
20.12	-8.00	0.5260	-0.0154	0.0933	0.0055	0.0144	0.0778	0.0779	0.0653	0.0125	-0.0001	0.661	0.0002	0.0154	0.4671	0.2540	1.839
20.12	-7.00	0.5273	-0.0153	0.0801	0.0051	0.0123	0.0775	0.0776	0.0651	0.0125	-0.0001	0.661	0.0006	0.0133	0.4684	0.2542	1.843
20.12	-6.00	0.5276	-0.0149	0.0674	0.0047	0.0104	0.0773	0.0773	0.0649	0.0125	-0.0001	0.660	0.0008	0.0114	0.4688	0.2541	1.845
20.12	-5.00	0.5274	-0.0138	0.0549	0.0040	0.0088	0.0770	0.0771	0.0647	0.0124	-0.0001	0.660	0.0008	0.0096	0.4687	0.2538	1.847
20.12	-4.00	0.5267	-0.0129	0.0422	0.0039	0.0068	0.0764	0.0764	0.0640	0.0124	-0.0001	0.659	0.0013	0.0077	0.4682	0.2529	1.851
20.12	-3.00	0.5263	-0.0116	0.0295	0.0038	0.0046	0.0772	0.0773	0.0649	0.0124	-0.0001	0.658	0.0020	0.0056	0.4676	0.2536	1.843
20.12	-2.00	0.5246	-0.0087	0.0180	0.0031	0.0027	0.0798	0.0799	0.0675	0.0124	-0.0001	0.656	0.0020	0.0036	0.4651	0.2555	1.820
20.13	-1.00	0.5247	-0.0081	0.0084	0.0014	0.0012	0.0799	0.0800	0.0676	0.0124	-0.0001	0.656	0.0009	0.0016	0.4651	0.2556	1.819
20.13	0.00	0.5245	-0.0081	-0.0013	-0.0002	-0.0004	0.0796	0.0797	0.0672	0.0124	-0.0001	0.656	-0.0001	-0.0005	0.4650	0.2553	1.822
20.13	1.00	0.5247	-0.0082	-0.0108	-0.0018	-0.0019	0.0798	0.0799	0.0675	0.0124	-0.0001	0.656	-0.0011	-0.0024	0.4651	0.2556	1.820
20.13	2.00	0.5252	-0.0088	-0.0196	-0.0036	-0.0033	0.0799	0.0800	0.0676	0.0124	-0.0001	0.656	-0.0022	-0.0043	0.4656	0.2559	1.819
20.13	3.00	0.5269	-0.0118	-0.0310	-0.0043	-0.0052	0.0776	0.0777	0.0653	0.0124	-0.0001	0.658	-0.0022	-0.0064	0.4680	0.2544	1.840
20.14	4.00	0.5279	-0.0133	-0.0440	-0.0044	-0.0074	0.0767	0.0768	0.0645	0.0124	-0.0001	0.659	-0.0016	-0.0085	0.4692	0.2539	1.848
20.14	5.00	0.5285	-0.0141	-0.0573	-0.0045	-0.0095	0.0770	0.0771	0.0648	0.0123	-0.0001	0.660	-0.0009	-0.0105	0.4696	0.2543	1.847
20.14	6.00	0.5295	-0.0152	-0.0706	-0.0051	-0.0113	0.0773	0.0774	0.0651	0.0123	-0.0001	0.661	-0.0009	-0.0124	0.4705	0.2549	1.845
20.14	7.00	0.5293	-0.0154	-0.0833	-0.0054	-0.0132	0.0776	0.0777	0.0655	0.0122	-0.0001	0.661	-0.0005	-0.0143	0.4702	0.2553	1.842
20.15	8.00	0.5282	-0.0154	-0.0962	-0.0057	-0.0153	0.0781	0.0781	0.0659	0.0122	-0.0001	0.661	-0.0001	-0.0163	0.4689	0.2553	1.837
20.15	9.00	0.5273	-0.0149	-0.1092	-0.0064	-0.0171	0.0790	0.0790	0.0668	0.0123	-0.0001	0.660	-0.0001	-0.0183	0.4678	0.2559	1.828
20.16	10.00	0.5249	-0.0140	-0.1220	-0.0071	-0.0189	0.0799	0.0800	0.0676	0.0124	-0.0001	0.660	-0.0001	-0.0202	0.4652	0.2559	1.818

DCY/DBETA=-0.0094 DCLN/DBETA=-0.0017 DCLL/DBETA=-0.0015

PHOTOGRAPH TAKEN AT BETA = -10.07 -5.06 -0.09 4.95 9.99

Sample Tabulated Body and Stability Axes
Aerodynamic Coefficients

SUPPLEMENTARY

INFORMATION

Corrected Page

5.0 REFERENCES

1. Test Facilities Handbook (Tenth Edition), "von Kármán Gas Dynamics Facility, Vol. 3," Arnold Engineering Development Center, May 1974.

2. "Aerodynamic Design Data Book - Vol. 1, Orbiter Vehicle," SD72-SH-0060-1K, Rockwell/Space Division, November 1977.